

Provolution in the Feature-Optical Grating

Paul Mirsky

paulmirsky633@gmail.com

May 22, 2020

Abstract

Features in the propagating grating may be inclined to either width or depth. We propose general rules that govern feature inclination, and show how these rules apply in a diverse set of example cases. We also give inductive formulas to parameterize light patterns, which approximately match the results calculated from first principles in earlier work.

1 Introduction

Feature Optics (FO) was recently introduced in a series of papers^{1,2,3,4,5}. FO describes diffraction and interference in terms of bright and dark *features*, which represent the spatial symmetries and asymmetries of light patterns. FO has been applied to two paradigmatic patterns – the simple beam and the grating.

Reference 4 postulated principles of *glow* and *shine*, and showed how a simple algorithm can apply these to compute the patterns in grating planes. Reference 5 introduced the concept of *provolution* and applied it to the simple beam. In this work, we draw upon both of these references to show how provolution works in the grating.

Provolution is the process by which one light pattern transforms into another as the light propagates. It is analogous to the Fractional Fourier Transform in conventional optics^{6,7,8}. If an initial flat wavefront has pattern $r(x)$, then its Fourier Transform $FT[r(x)]$ appears in the far field or in the rear focal plane of a lens. FO describes this as a change of *inclination*, which can vary from wide to deep.

This work begins by adapting the rules of inclination to the case of the grating. Later, we step through all the critical planes of the grating, and show how the rules for inclination apply at each plane. We also compare the results with those calculated in Reference 4.

This work assumes that the reader is completely familiar with references 1– 5.

2 Rules for discrete inclination

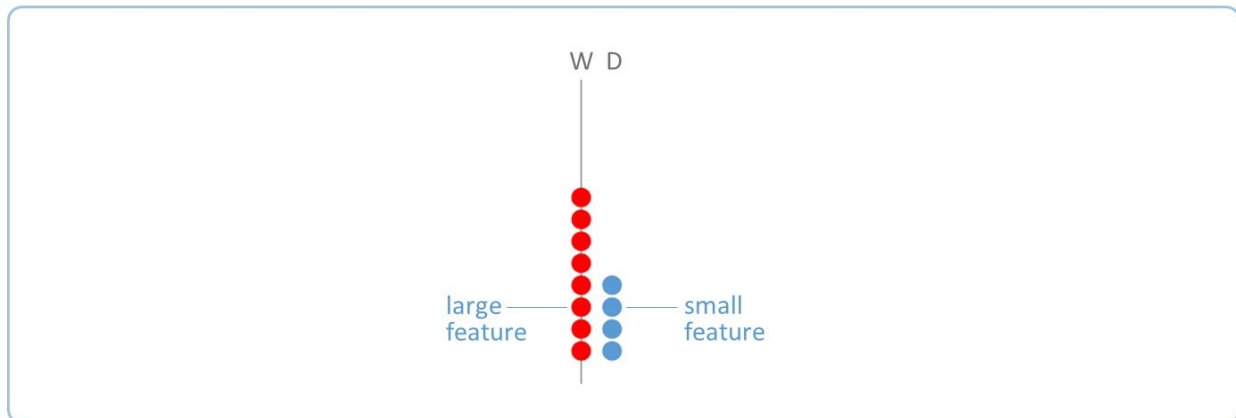
2.1 The simple beam

Reference 5 described the principles of inclination in the simple beam. While inclination can actually take a continuous range of values, feature diagrams employ a discrete approximation in which there are only two possible inclinations: wide and deep. In this work we consider only these two possibilities, for the sake of conceptual simplicity.

The rule governing beam inclination may be summarized as:

The beam consists of two bright features: the glow and the shine. The *larger* one is inclined wide, while the *smaller* one is inclined deep (see Figure 2.1).

Figure 2.1, Inclination in the beam



Dark features do not count towards this rule; only bright features do. Also note that when glow and shine are the same size, we draw the shine wide by convention.

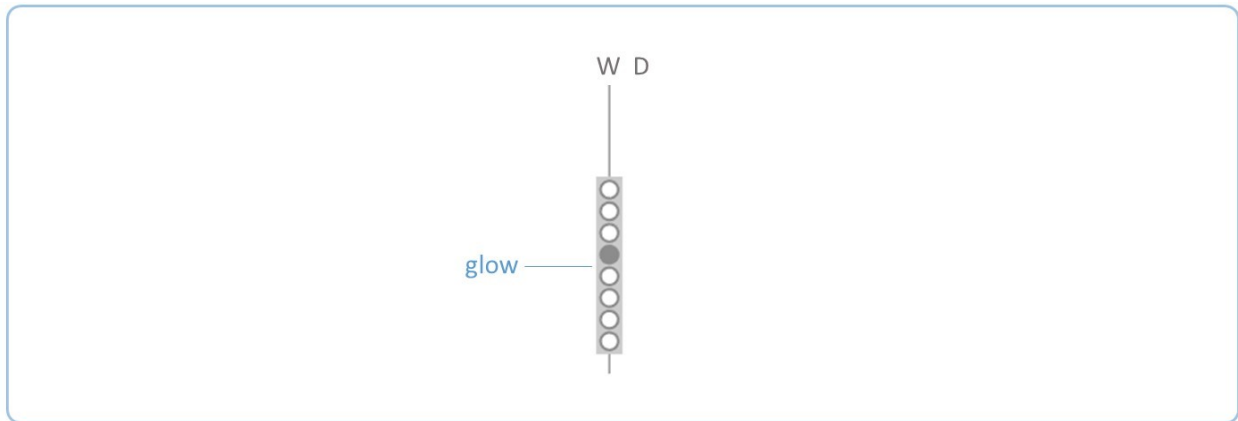
In the following sections of this chapter we adapt this rule to the grating, in which glow and shine are each a ranked chain of features, rather than just a single feature. The set of possible cases is much wider; accordingly, the grating rules are substantially more complicated.

Different ranks may have different inclinations. The rules below apply to an individual rank, or to a set of adjacent ranks that are connected by overlapping features.

2.2 Rule 1: glow only

If there is only one feature at a given rank, it can only be a glow feature, and it is inclined wide (see Figure 2.2).

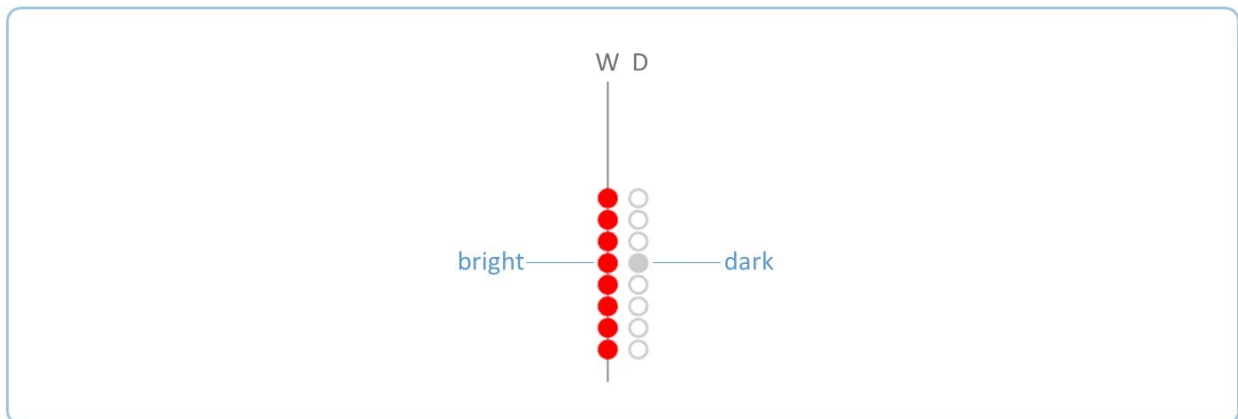
Figure 2.2, Inclination rule 1



2.3 Rule 2: bright and dark feature

If one feature is bright and the other is dark, the bright feature is inclined wide and the dark feature is inclined deep (see Figure 2.3). The rule applies regardless of which feature is glow and which is shine.

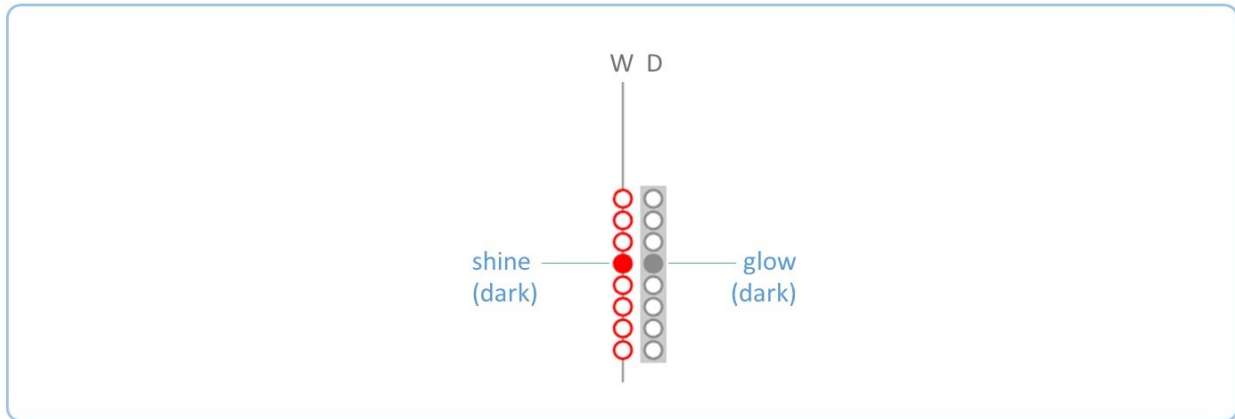
Figure 2.3, Inclination rule 2



2.4 Rule 3: two dark features

If both features are dark, the shine is inclined wide, and the glow is inclined deep (see Figure 2.4).

Figure 2.4, Inclination rule 3



This rule is really just a convention rather than a physical principle; there would be no physical consequence of consistently using the opposite convention. It exists mainly to eliminate the ambiguity of an undefined case.

2.5 Rule 4: bright features, fully overlapped

If both features are bright and one *fully overlaps* the other, then the large feature is inclined wide, while the small one is inclined deep (see Figure 2.5).

Figure 2.5, Inclination rule 4



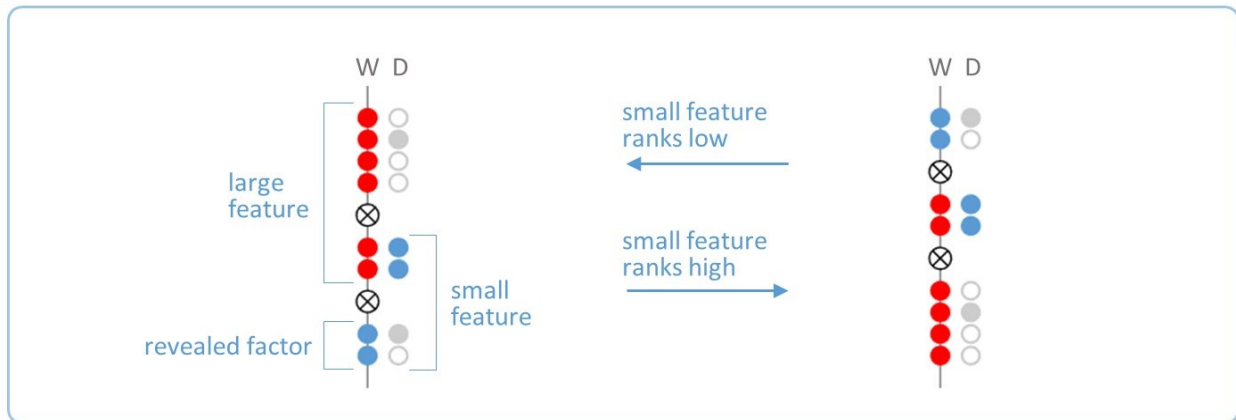
This is fundamentally the same as the single rule which governs inclination in the simple beam. It applies regardless of whether the small feature ranks at the top of the large feature, or at the bottom.

In this scenario, there is typically also a dark feature ranked above or below the small feature; it is inclined deep.

2.6 Rule 5: bright features, partially overlapped

If both features are bright and they *partially overlap* in rank, then the large feature is again inclined wide, and the overlapped portion of the small one is inclined deep (Figure 2.6). The revealed factor of the small feature (the portion that does not share its rank with any bright feature) is inclined wide.

Figure 2.6, Inclination rule 5

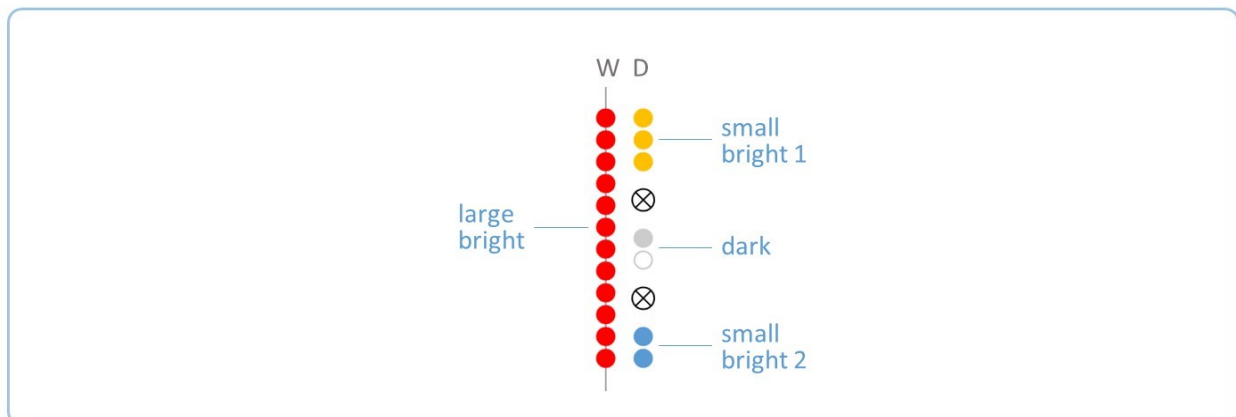


This rule applies regardless of which is glow or shine, and regardless of which is at higher rank.

2.7 Rule 6: multiple bright features

If a single bright feature shares a rank with multiple bright features separated by a dark feature, then the single feature is larger and is inclined wide, while both smaller features are inclined deep (see Figure 2.7).

Figure 2.7, Inclination rule 6



This rule is actually a corollary to rule 4, because the two small bright features combined are equivalent to one medium-sized feature that is nevertheless smaller than the large feature.

3 Breaking cases and sprouting cases

A grating is uniquely parameterized by four different numbers – A, B, C, and D, which are the sizes of the corresponding features A, B, C, and D, from low rank to high. All parameters are greater than 1, and typically $D \geq A \cdot B \cdot C$. This permits a very large parameter space of possible gratings, some of which have fundamental differences; however, many of these possibilities are qualitatively identical to others.

The parameter space can be divided into 10 qualitatively different cases, listed in Figure 3.1. They vary in two different ways: by *breaking* case, and by *sprouting* case.

Figure 3.1, Parameter cases

ID	breaking case	early elbow sprouting case	core start sprouting case	medial sprouting case
1	early ($B > C$)	before array ($A < B$)	before texture ($A < C$)	after texture ($A > C/B$)
2	early ($B > C$)	before array ($A < B$)	after texture ($A > C$)	after texture ($A > C/B$)
3	early ($B > C$)	before texture ($A > B, A < BC$)	after texture ($A > C$)	after texture ($A > C/B$)
4	early ($B > C$)	after texture ($A > BC$)	after texture ($A > C$)	after texture ($A > C/B$)
5	late ($B < C$)	before array ($A < B$)	before texture ($A < C$)	before texture ($A < C/B$)
7	late ($B < C$)	before array ($A < B$)	before texture ($A < C$)	after texture ($A > C/B$)
6	late ($B < C$)	before texture ($A > B, A < BC$)	before texture ($A < C$)	before texture ($A < C/B$)
8	late ($B < C$)	before texture ($A > B, A < BC$)	before texture ($A < C$)	after texture ($A > C/B$)
9	late ($B < C$)	before texture ($A > B, A < BC$)	after texture ($A > C$)	after texture ($A > C/B$)
10	late ($B < C$)	after texture ($A > BC$)	after texture ($A > C$)	after texture ($A > C/B$)

There are two different breaking cases. In the *early-breaking* grating, breakout occurs at or before the medial. In the *late-breaking* grating, breakout occurs at or after the medial. These are equivalent to the cases $B \geq C$ and $B \leq C$, respectively. The *medial-breaking* case occurs when $B = C$, and it can be treated as either early- or late-breaking. Previous work⁴ has treated only the late-breaking case.

Each shape of the shine – form, array, and texture – *sprouts* at the plane where it grows to 1 patch in size. The shapes sprout at Z values of A, A·B, and A·B·C, respectively. Before a shape sprouts, it can have no physical effect. In each critical plane, various sprouting cases may be possible – for example, the medial (rightmost column in Figure 3.1) may occur before the texture has sprouted, or after the texture has sprouted; in all cases, the medial occurs after the form and array have sprouted.

This work will analyze all the cases in the table above. To prevent a proliferation of further sub-cases, we will not consider examples in which a feature sprouts in the middle of any stage; any feature which sprouts by the final plane, will have sprouted by the first plane.

Note that different sprouting case do not have different patterns in width – i.e. the observable texture, array, and form shapes. Sprouting case affects only the depth of the pattern.

4 Computing the symmetry

Reference 4 introduced the principles of calculating patterns from glow and shine. These were implemented in an algorithm which fills arrays of cells to produce *tracked-shine diagrams*. This work will describe patterns instead using *spatial-symmetry diagrams*, which are derived from tracked-shine diagrams following the steps drawn in Figure 4.1.

Figure 4.1, From tracked shine to spatial symmetry

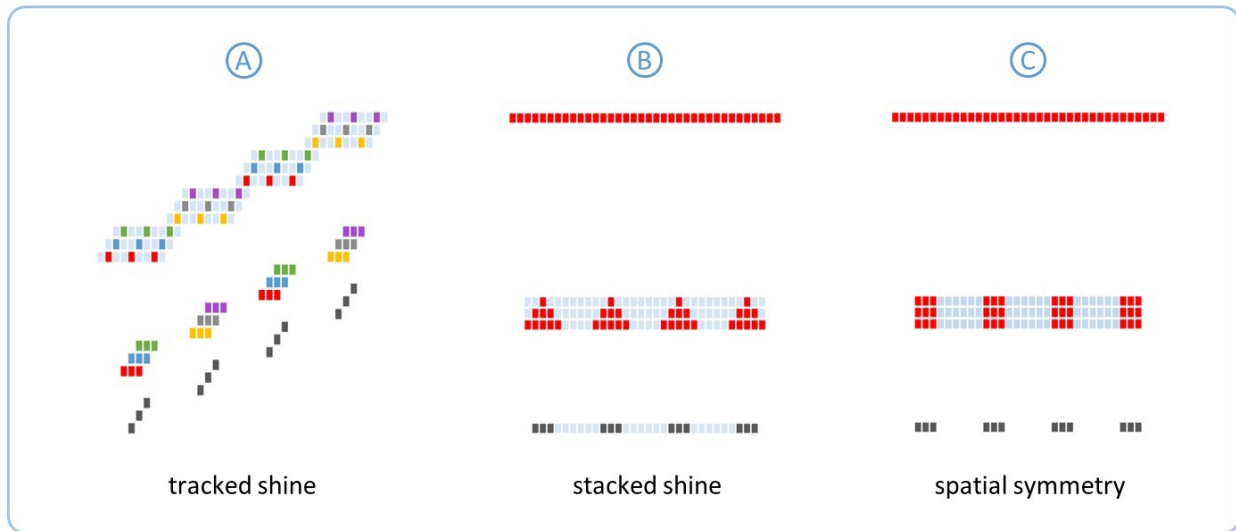


Figure 4.1a shows a typical tracked-shine diagram. Each shine instance is drawn in a different coded color and staggered vertically, which lets the user ‘track’ the shine emanating from each source patch. It is simplified to a *stacked-shine diagram* as shown in Figure 4.1b by rendering all bright shine in one color, effectively erasing the information about the source of each patch.

The number of bright patches and their spatial locations are retained. Dark shine is not counted; it is optionally retained in the diagram as a way to show the width and location of the empty space, but the depth of the dark shine is not physically meaningful and should not be interpreted. When bright and dark shine both appear in the same target patch (column), the combination appears bright and the dark shine is not observable. Dark space is only observable at a target patch that receives *only* dark shine, or one that receives no shine at all.

The spatial-symmetry diagram, shown in Figure 4.1c, is an approximation of the stacked-shine diagram. The diverse and often complicated patterns of the stacked-shine diagram are replaced by basic rectangles of equivalent sizes. This greatly simplifies the patterns to their conceptual essence, while preserving their width and depth symmetries.

The spatial-symmetry diagrams are not computed directly from the stacked shine, but rather from *inductive formulas*. These formulas were not derived rigorously from first principles; instead, they were determined inductively by experimenting with many examples of stacked-shine diagrams and generalizing simple rules that match the stacked-shine diagrams to a good approximation.

While this process of discovery is inscrutable, it is easy to verify that the resulting formulas work by simply testing many examples. The companion code for this work is available at Github⁹ for the reader to use, test, and modify. The outputs of many tests are also available in pdf form in the Github repository. When determining that two different patterns ‘match’, three rules apply: First, the formula depth of a pattern is equal to the *maximum depth* in the stacked-shine diagram. Second, when the stacked shine is a triangle or trapezoid, the formula width matches the *half-max width* in the stacked-shine diagram – in other words, truncate the width at the point where its depth is half of its maximum value. Third, the stacked-shine depth is actually the product of the texture depth and the form depth; their half-max points must be determined separately.

5 Provolution by wide and deep inclinations

5.1 Overview

In this chapter, we apply the rules for discrete inclination to all the critical planes, treating each sprouting and breaking case separately. Note that the medial plane is presented *before* breakout, which matches the late-breaking case; so, the early-breaking case is presented out of its actual physical order.

Each section contains three main diagrams. First it contains a feature diagram with width and depth columns to indicate inclination, as introduced in reference 5. Note that these diagrams are easily confused with the different style of feature diagram used in reference 4; in those, the two columns represent glow and shine, rather than width and depth.

Second, each section contains one spatial-symmetry diagram showing the first and last planes of the stage with all bright features identified, including their inclinations. These planes mark the endpoints of a trend which occurs over the course of the stage as features grow, rise in rank, and provolve.

Third, each section contains a second spatial-symmetry diagram showing many planes as well as a formula for the symmetries. These formulas often take parameter p , which denotes the size of the growing shine feature for that stage, which occupies the lowest rank and ultimately propels all other trends. Value p always begins at 1 at the first plane of every stage, and grows to some value p_{Max} at the last plane of the stage. Note that p is often only one factor of some larger feature, which had already sprouted in some earlier stage.

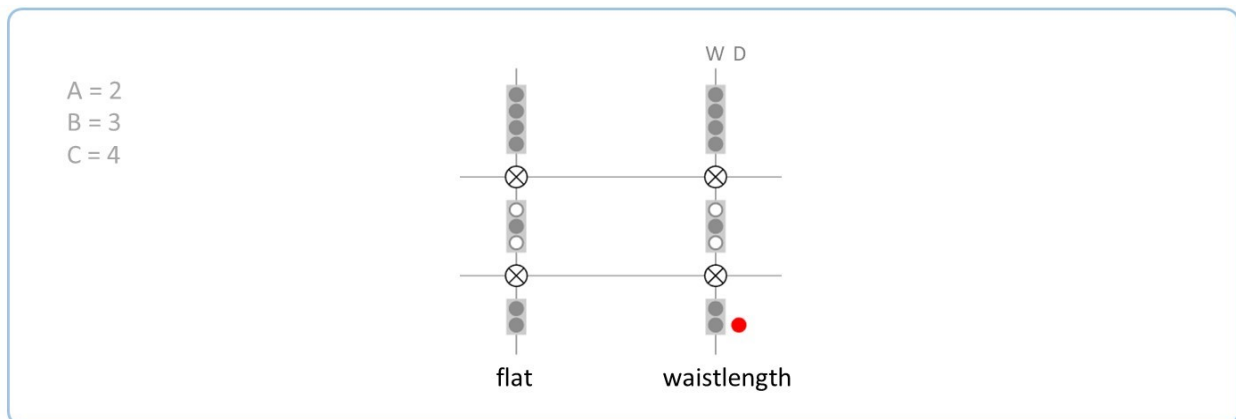
5.2 Flat and waistlength

We treat the flat as the starting plane. In practice, it is easy to set any initial pattern in this plane by illuminating an absorption grating with a wide coherent source.

In all stages except for this one, the pattern's total symmetry is the product of the bright glow and the bright shine. However, at the flat the shine is equal to zero. The smallest possible symmetry group consists solely of the identity element, with a size of 1, so a symmetry of zero does not make physical sense. Therefore, we compute the symmetry in this stage as if the shine were equal to 1.

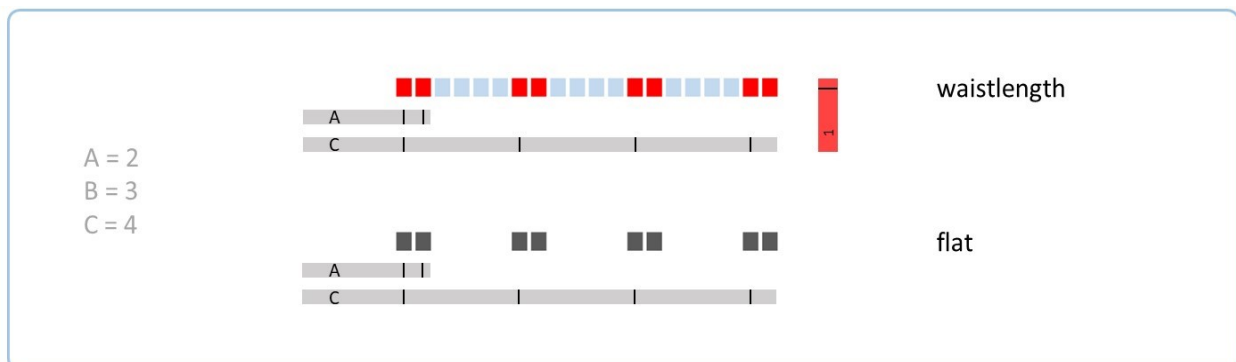
Likewise, we consider the depth at the flat to be equal to 1, i.e. a single patch, because a shallower depth is not possible. However, the first patch of shine does not fully sprout until the waistlength.

Figure 5.1, Feature diagram



- At the flat, all features are wide (rule 1).
- At the waistlength, all glow features remain wide, but shine is deep (rule 2).

Figure 5.2, Spatial-symmetry diagram

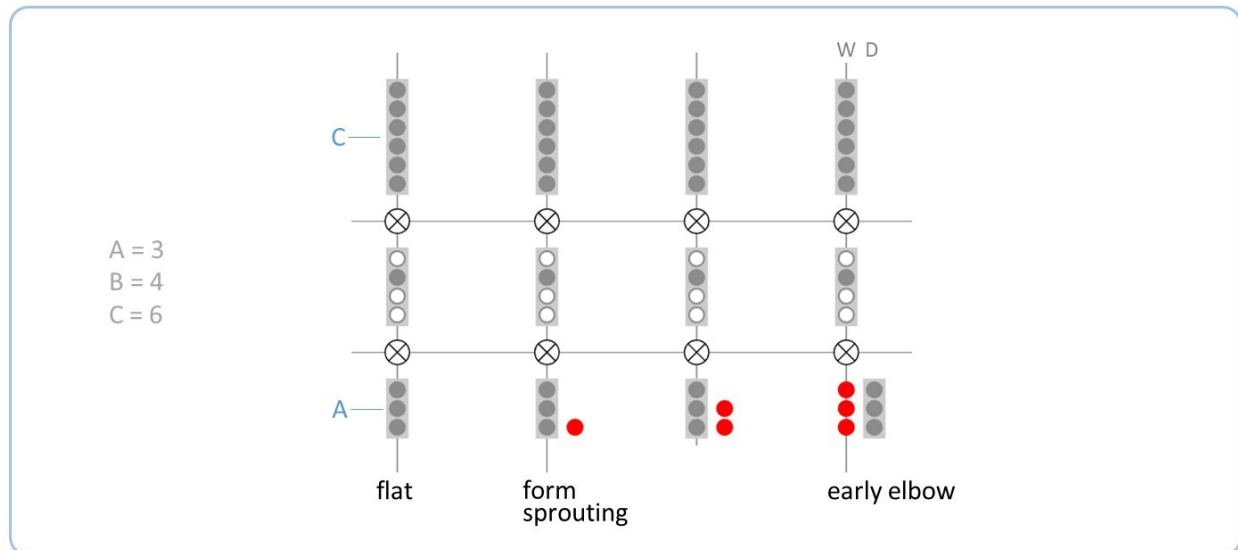


5.3 Early elbow

5.3.1 Sprouting case 1, before array

- This case occurs when $A \leq B$. Only bright shine has sprouted.
- This case is rare in practice, because it requires very small slits and/or a very large dark factor.

Figure 5.3, Feature diagram



- Inclination is as in the simple beam.
- At form sprouting, the shine is smaller than glow A. Therefore, shine is deep and glow is wide (rule 4).
- Form sprouting plane is also the waistlength.
- At early elbow, shine reaches the size of the glow. In the discrete approximation, glow and shine exchange inclination (rule 4).
- Feature C remains wide throughout, because it is the only feature at its rank (rule 1).

Figure 5.4, Spatial-symmetry diagram at endpoints

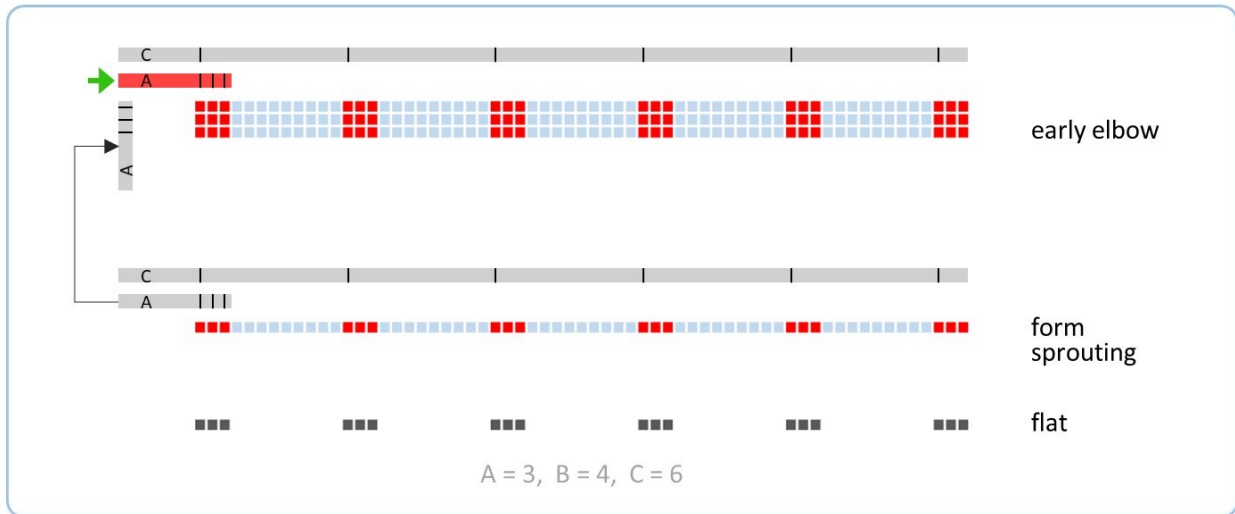
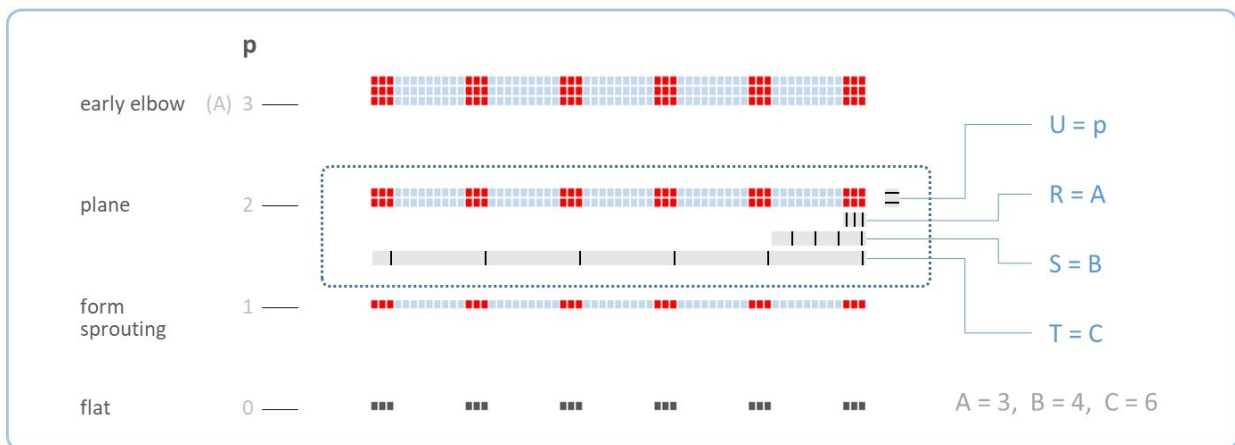


Figure 5.5, Inductive formulas

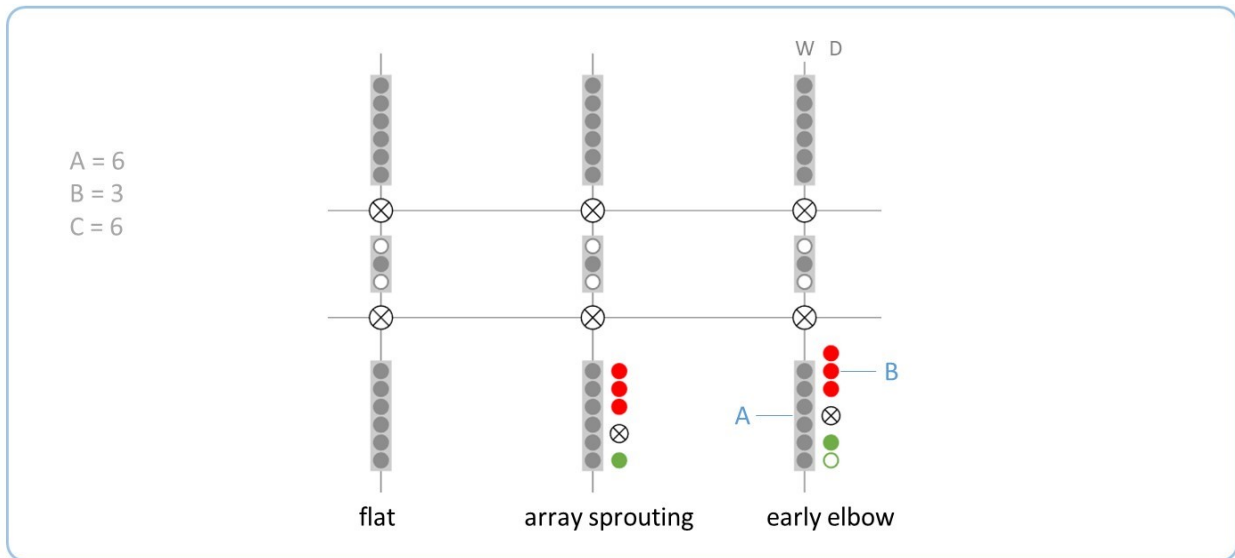


- In this and the other early elbow cases, the stage begins at a sprouting plane (here texture; form or array in the following cases). All subsequent stages begin at a critical plane.

5.3.2 Sprouting case 2, before texture

- In this case $A \geq B$, but $A \leq BC$.

Figure 5.6, Feature diagram



- Inclination is different from the simple beam, because the shine array sprouts before the early elbow. After the array sprouting, only dark shine grows and the pattern stops growing deeper with distance.
- $A \geq B$, so at the elbow feature A is wide, and B is deep (rule 4).

Figure 5.7, Spatial-symmetry diagram at endpoints

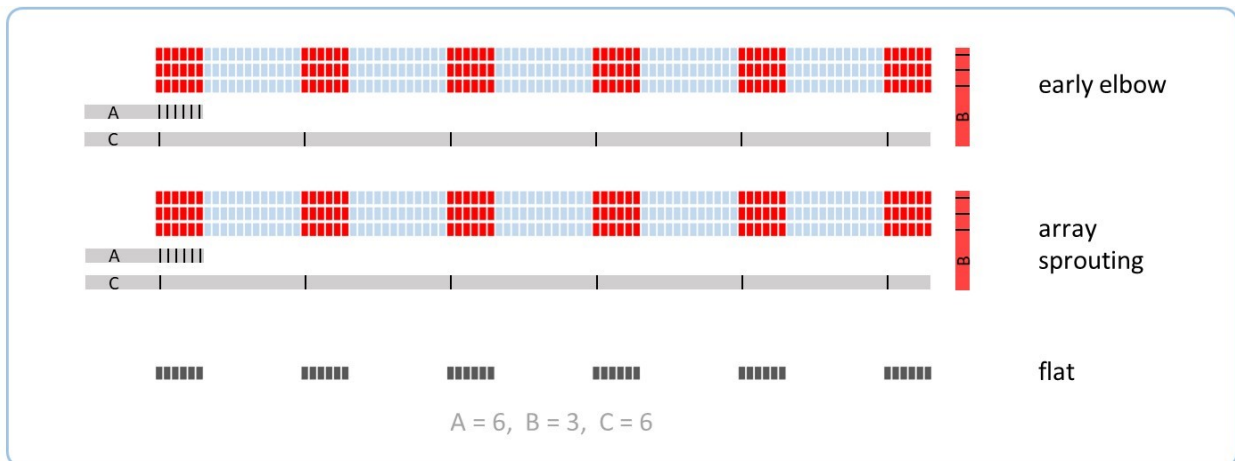
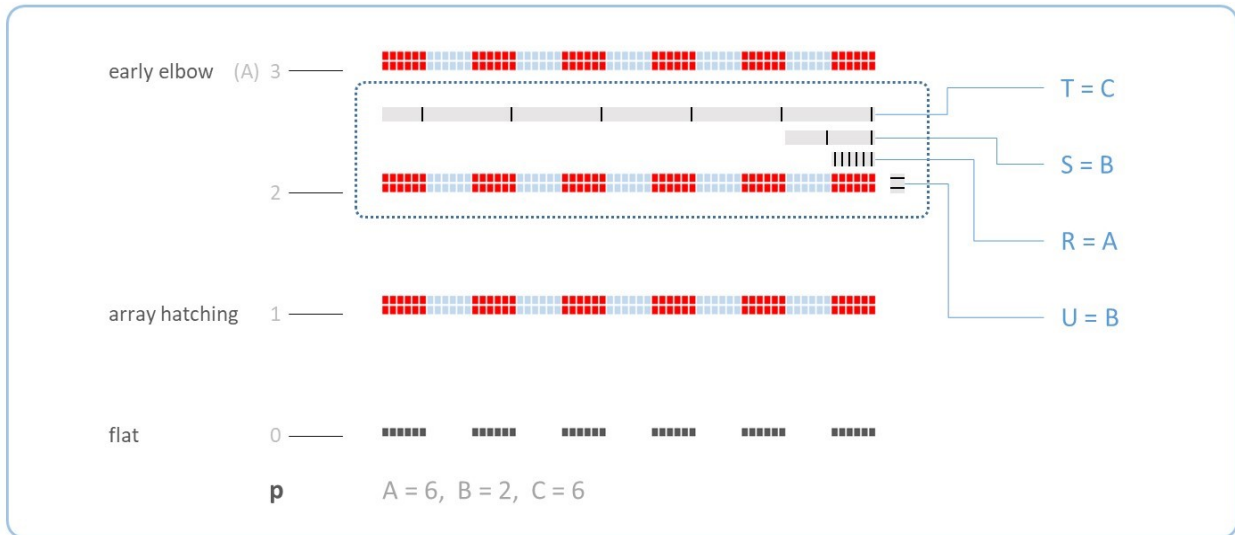


Figure 5.8, Inductive formulas

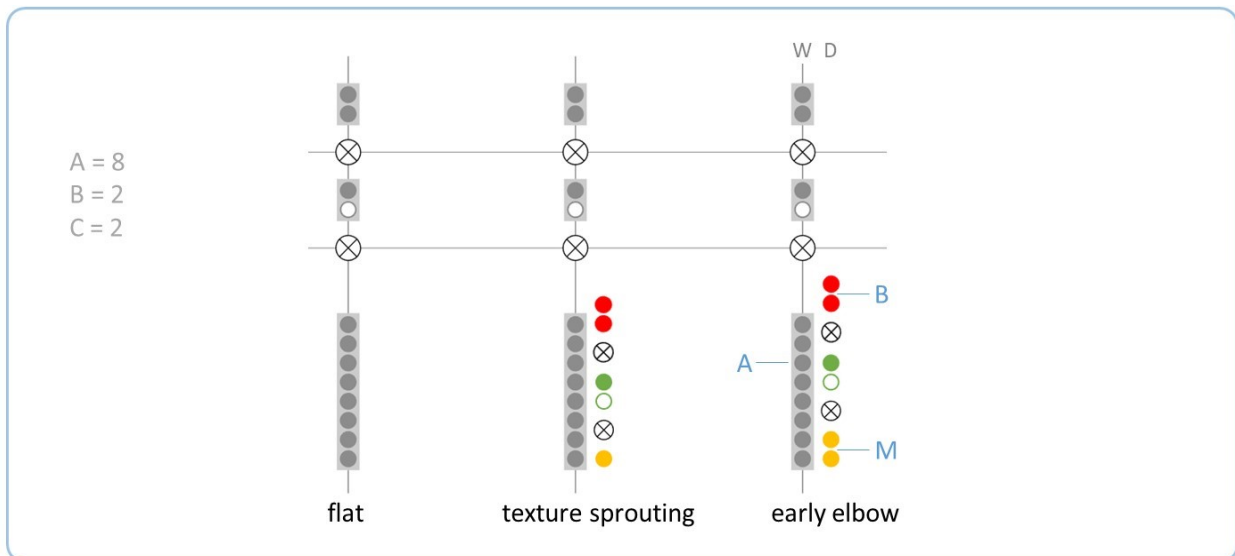


- The expanding dark shine does not change the symmetry at all.

5.3.3 Sprouting case 3, after texture

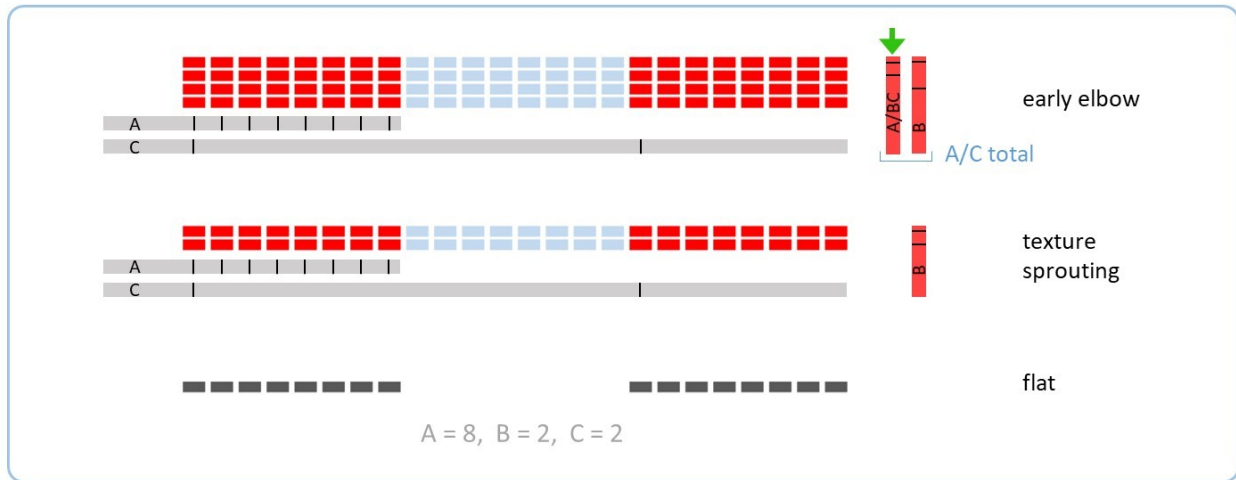
- In this case $A \geq BC$.

Figure 5.9, Feature diagram



- As in the previous case, A remains wide, while B and M are both deep (rule 6).

Figure 5.10, Spatial-symmetry diagram at endpoints



- As shine texture expands, depth grows proportionally to Z , reaching A/C at the early elbow. The dark shine acts as a 'hole' of size C , reducing the depth by a factor of C compared to the case of a simple beam (where depth = A).

Figure 5.11, Inductive formulas

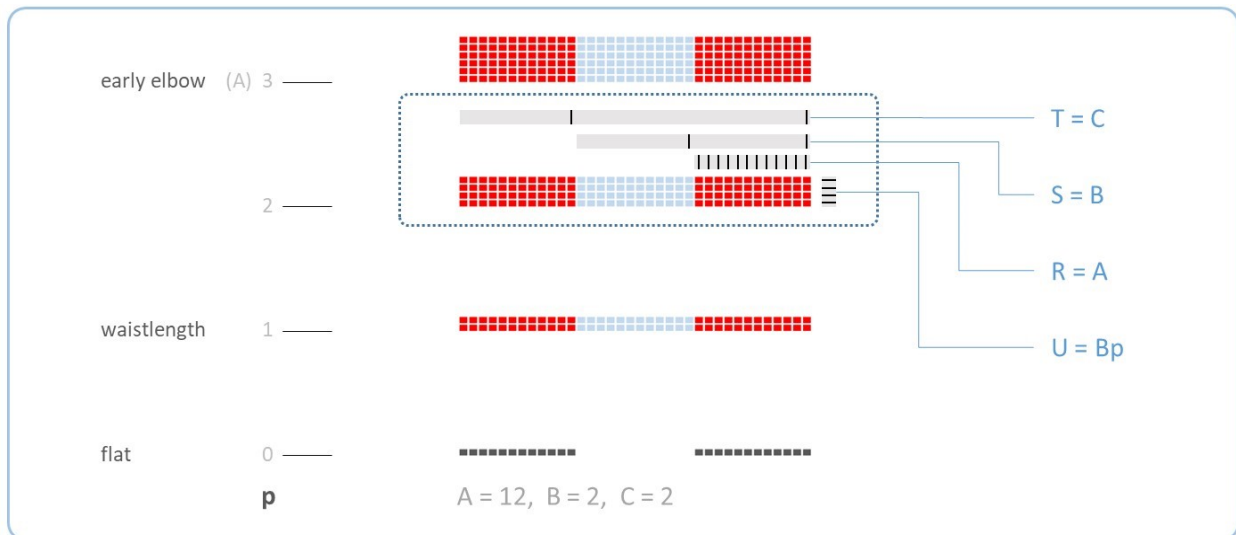
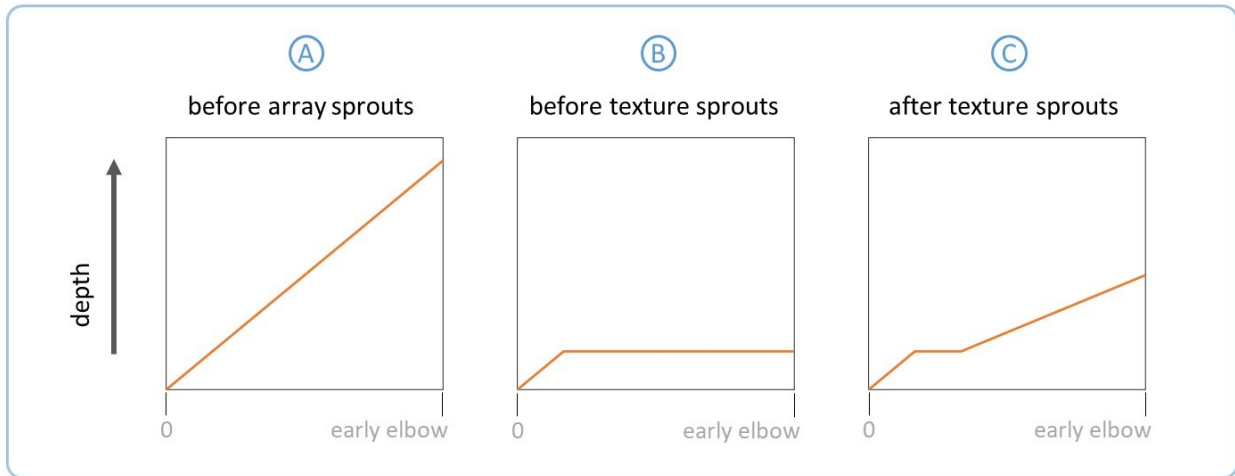


Figure 5.12 summarizes the trends in depth for all 3 sprouting cases. Subfigures a, b, and c correspond to sprouting cases 1, 2, and 3 respectively. The common governing principle is that depth grows linearly with Z whenever bright shine is growing, but remains at a constant plateau when dark shine is growing. Depth increases faster when the form is growing, and slower when the texture is growing.

Figure 5.12, Depth in various sprouting cases

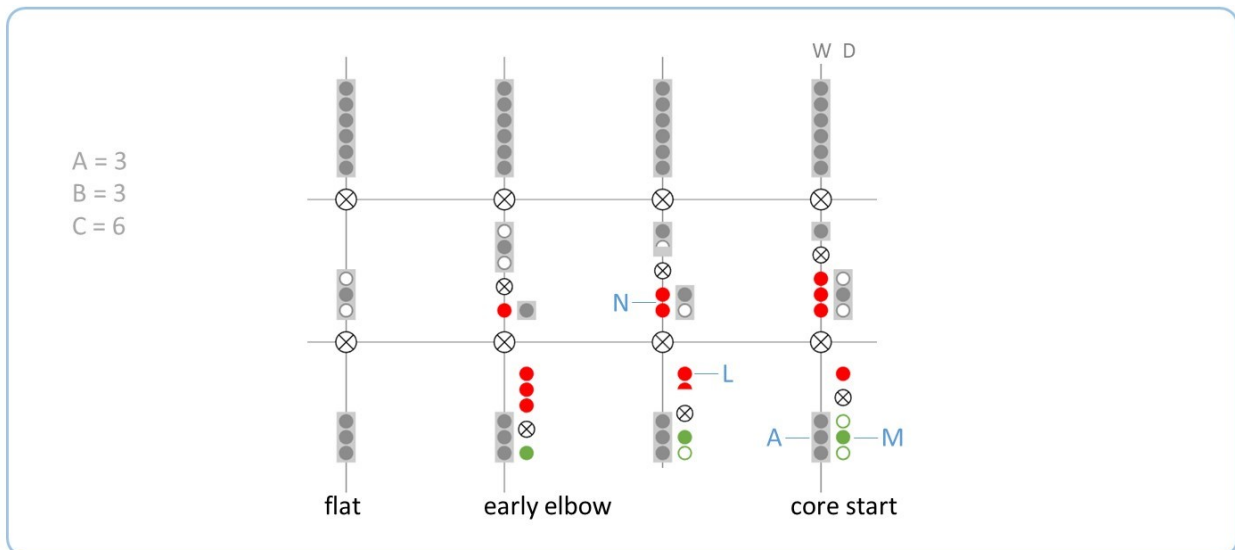


5.4 Core start

5.4.1 Sprouting case 1, before texture

- This sprouting case occurs when $A \leq C$. Equivalently, the shine texture has not sprouted at the core start.
- The formulas here are valid when array sprouts by early elbow, i.e. when $A \geq B$.

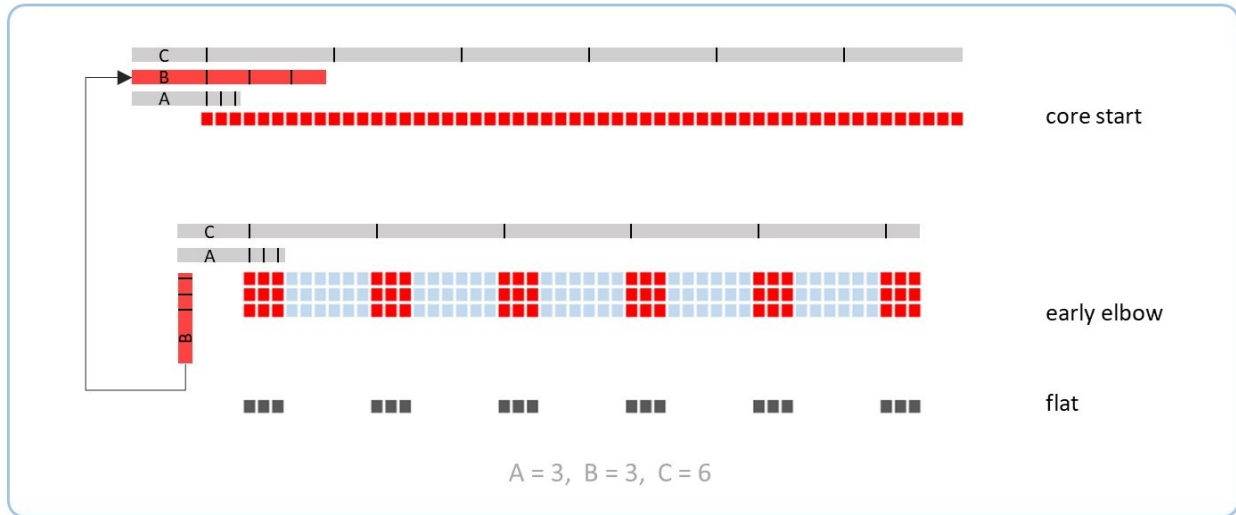
Figure 5.13, Feature diagram



- Only dark shine M ranks with glow feature A, so depth is trivial (depth = 1).
- Unlike in the simple beam where the entire wide area consists only of shine, here the wide area has both shine (N) and glow factors (A).

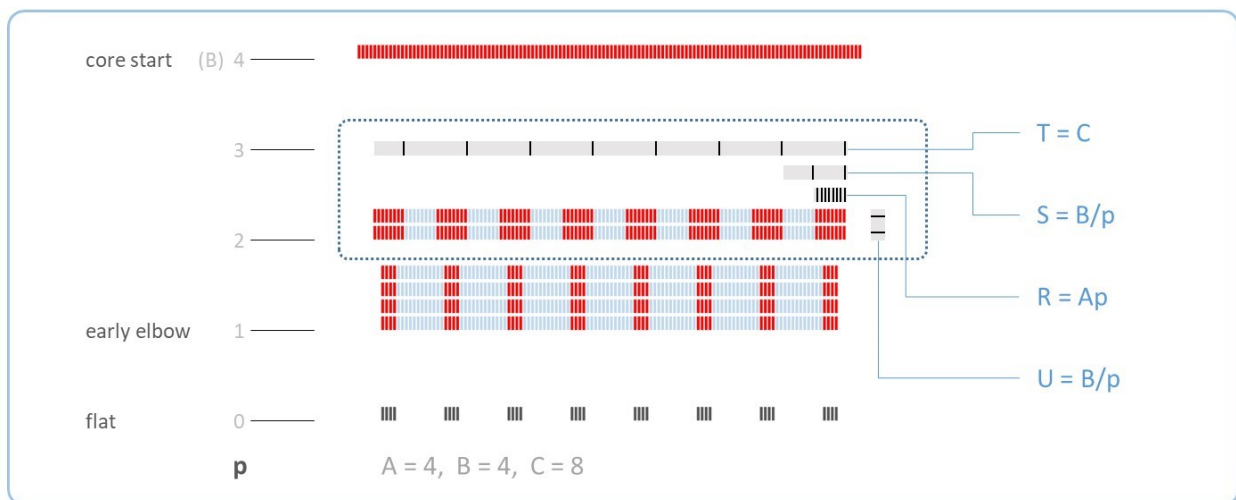
- The bright shine is divided between two factors: N, which ranks above A, and L, which ranks at the top of A. Factor N is wide (rule 5, rule 2). Because $A \geq B$, L is deep (rule 5).
- Note that in this particular example, the array sprouting plane coincides with the early elbow, but this is not generally true.

Figure 5.14, Spatial-symmetry diagram at endpoints



- Expanding dark shine is not directly visible in the diagram. It is visible indirectly, because bright shine provolves from deep to wide.
- Depth decreases by a factor of B, and width increases by the same factor.

Figure 5.15, Inductive formulas

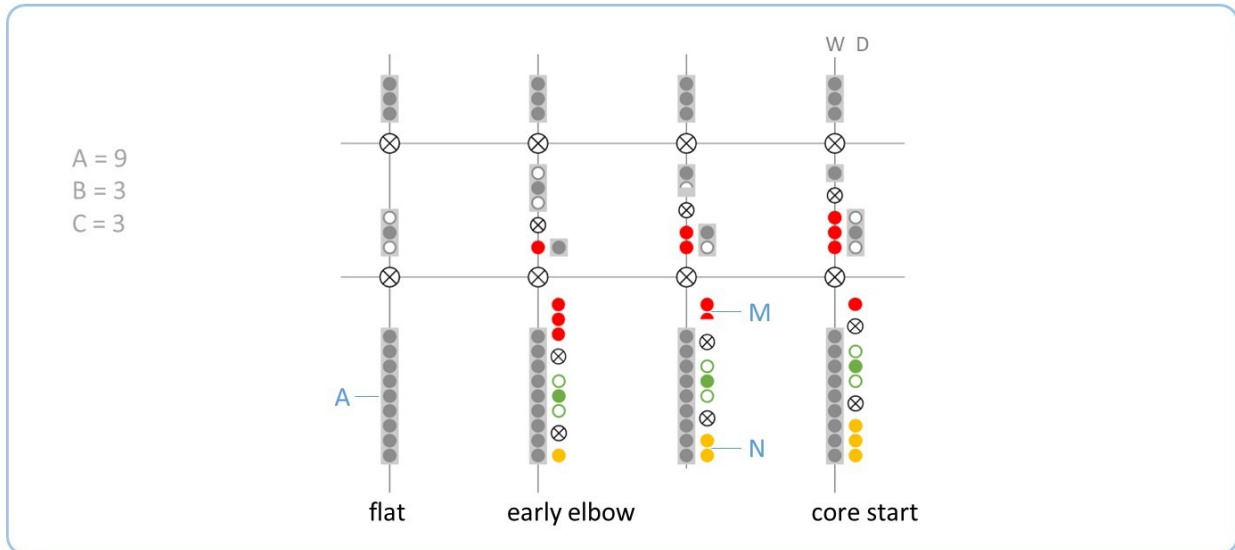


5.4.2 Sprouting case 2, after texture

- In this sprouting case, $A \geq C$. The shine texture sprouts before the core start.

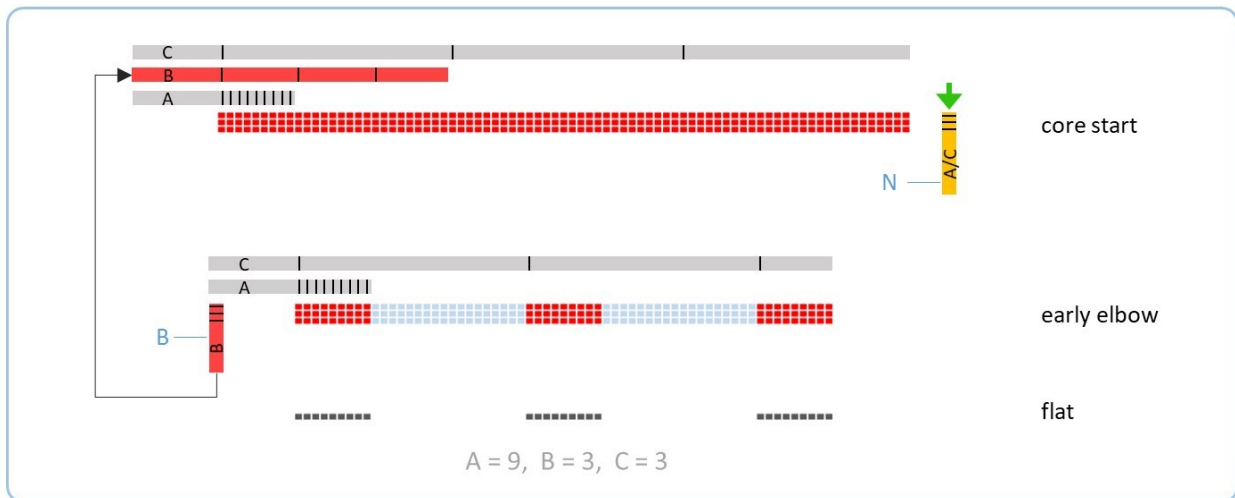
- This case is similar to the previous case, except that there is an additional bright feature N, as drawn in Figure 5.16.
- The formulas here are valid when texture sprouts by early elbow, i.e. when $A \geq BC$.

Figure 5.16, Feature diagram



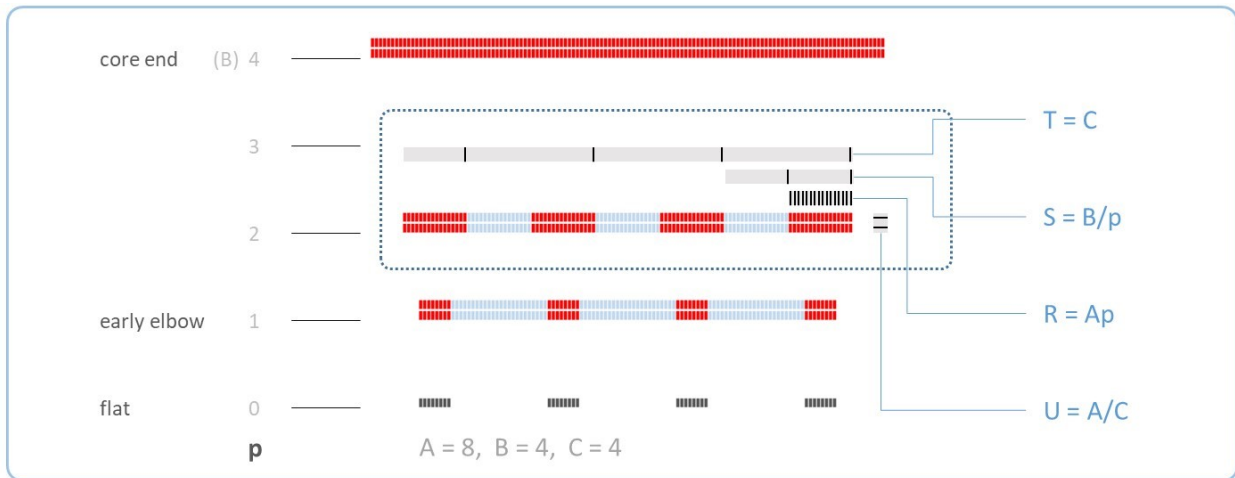
- Feature A is wide, because it is larger than the product of M and N (rule 6, rule 5).
- Note that in this example, the texture sprouting plane coincides with the early elbow, but this is not generally true.

Figure 5.17, Spatial-symmetry diagram at endpoints



- Feature N expands in depth, while equivalently-sized feature B *leaves* depth and is promoted to width at a higher rank.

Figure 5.18, Inductive formulas



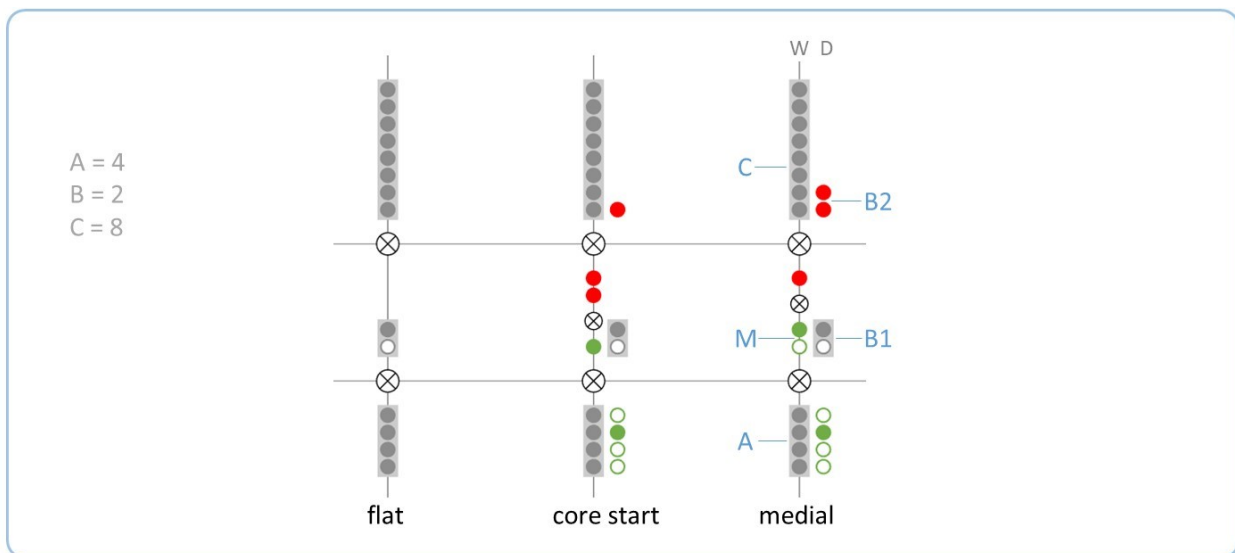
- Total depth remains constant.

5.5 Medial

5.5.1 Sprouting case 1, before texture / breaking case 1, late-breaking

- In this sprouting case $A \leq C/B$. At the medial, the shine array has sprouted but the shine texture has not.
- In this breaking case, $C \geq B$.

Figure 5.19, Feature diagram



- Feature A is wide because it ranks with a dark feature (rule 2).

- Dark shine factor M ranks with feature B1. Because there are two dark features at the same rank, the observable pattern appears dark. By rule 3, shine M is wide while glow B1 is deep; but, the inclination of dark features actually has no physical manifestation.
- At the highest rank, B2 ranks at the bottom of C. Because $C \geq B$, C remains wide while B2 provolves to depth (rule 4, rule 5).

Figure 5.20, Spatial-symmetry diagram at endpoints

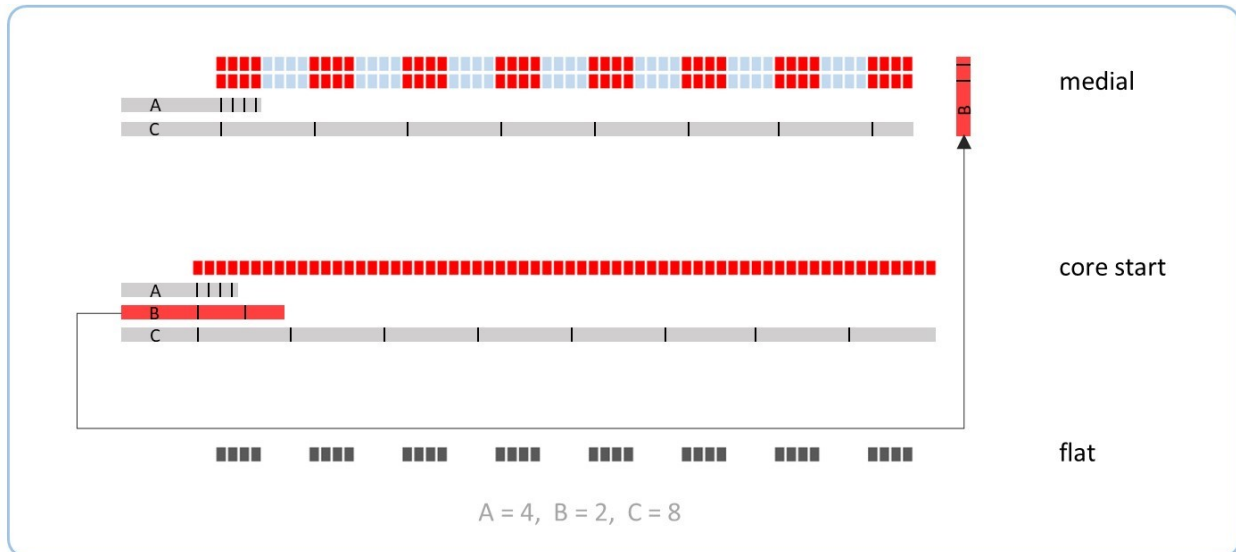
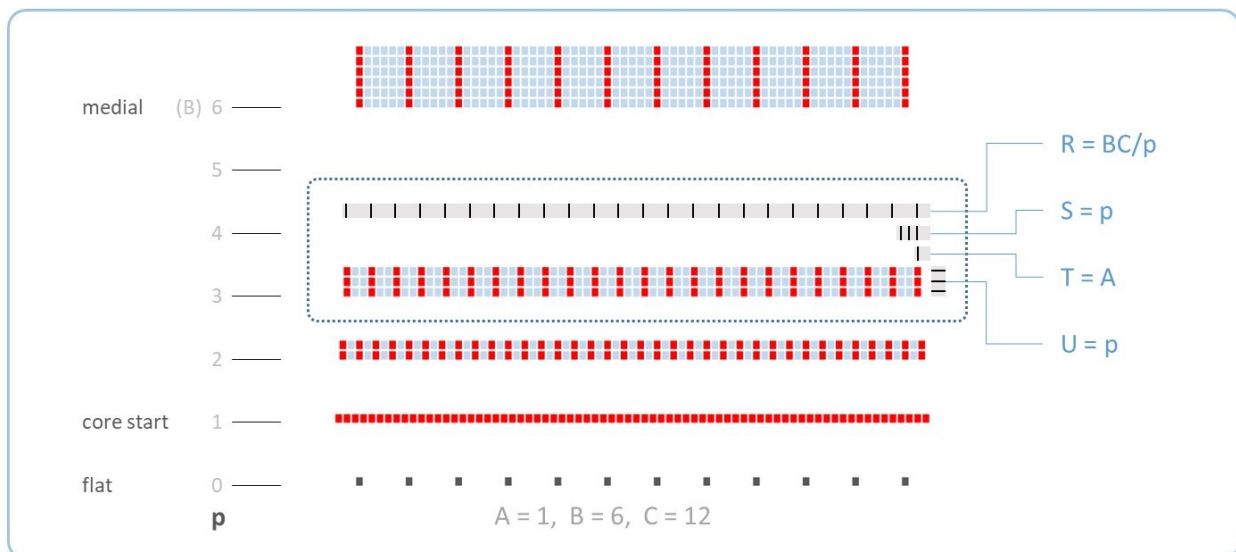


Figure 5.21, Inductive formulas

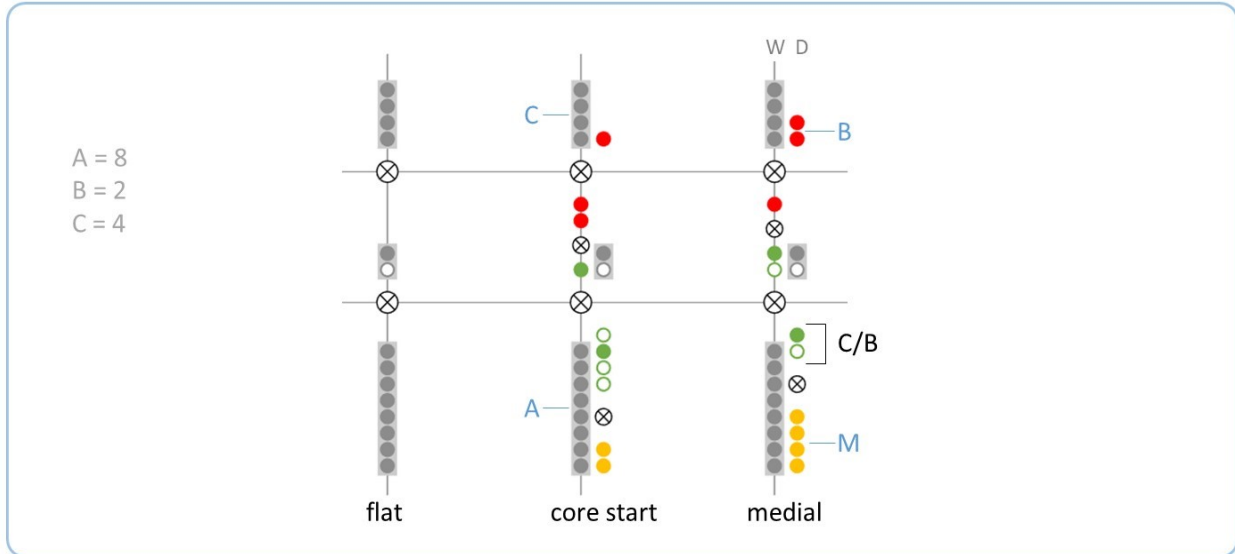


- Because feature A is wide, the early revivals and the medial all retain the texture of the starting pattern.
- The formulas in Figure 5.21 do *not* apply at all planes; they are valid only when B/p is an integer.

5.5.2 Sprouting case 2, after texture / breaking case 1, late-breaking

- This sprouting case occurs when $A \geq C/B$. The shine texture sprouts at or before the medial.
- The formulas here are valid when texture sprouts by core start, i.e. when $A \geq C$.
- This case is very similar to the previous case; the only difference is that the depth contains an additional factor M of size AB/C at the medial.

Figure 5.22, Feature diagram



- Feature A is larger than feature M, so A is wide while M is deep (rule 4).
- As in the previous case, B ranks at the bottom of C and is deep.

Figure 5.23, Spatial-symmetry diagram at endpoints

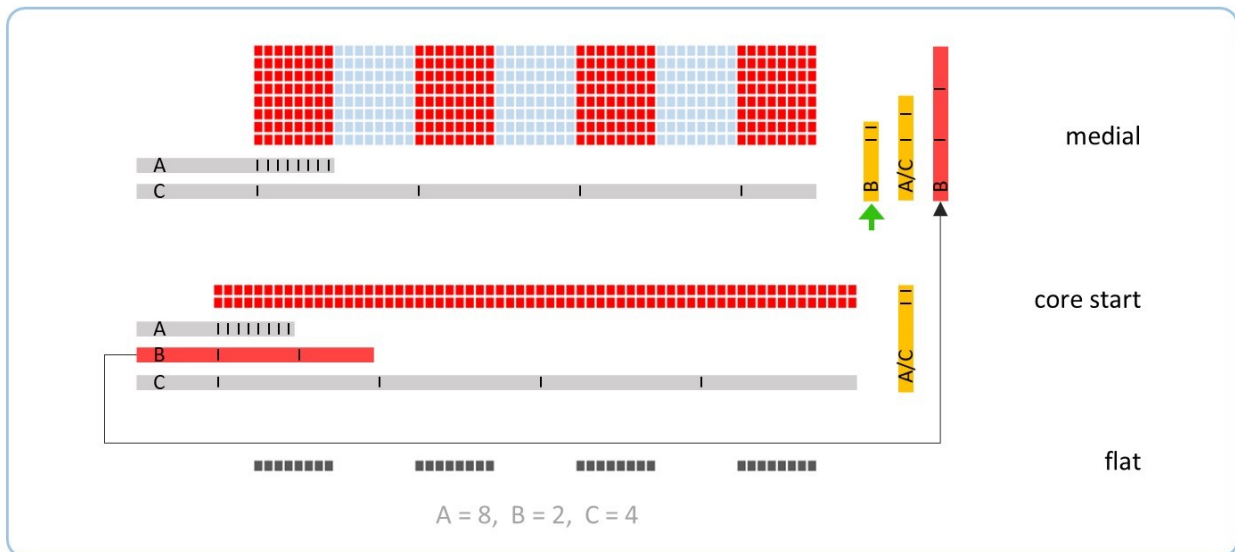
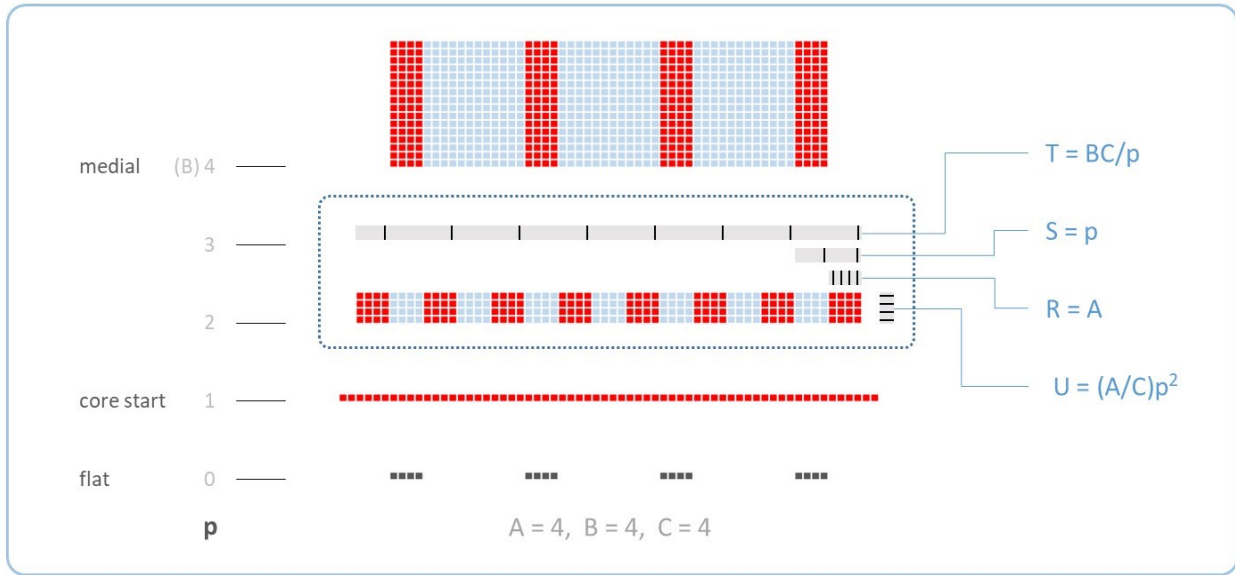


Figure 5.24, Inductive formulas

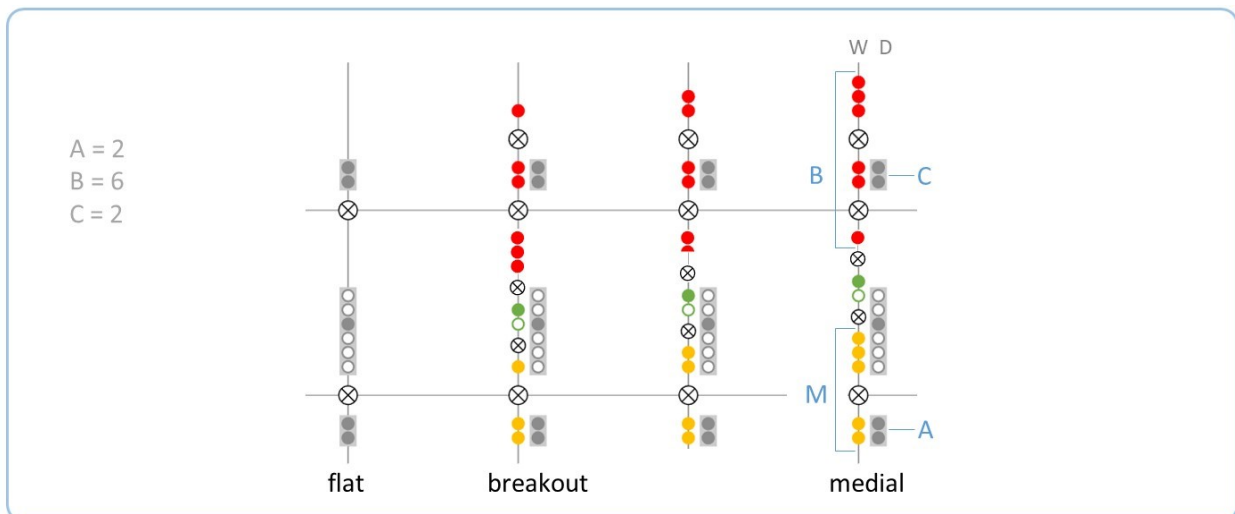


- As in the previous case, the formulas in Figure 5.24 do *not* apply at all planes; they are valid only when B/p is an integer.

5.5.3 Breaking case 2, early-breaking

- The previous two medial cases were both *late-breaking* gratings, i.e. $C/B \geq 1$. This case is the *early-breaking* grating in which $C/B \leq 1$.
- In this case, the medial plane actually occurs *after* breakout; note that this text presents these planes out of their actual order.
- All shine shapes have necessarily sprouted, and thus there is only one possible sprouting case.

Figure 5.25, Feature diagram



- Feature M is larger than A; thus, M is wide while A is deep (rule 4).
- Feature B is larger than C; thus, B is wide while C is deep (rule 4, rule 5).
- As B rises in rank, C moves from the top of B to the bottom of C. However, this does not affect inclination, because their relative sizes do not change.

Figure 5.26, Spatial-symmetry diagram at endpoints

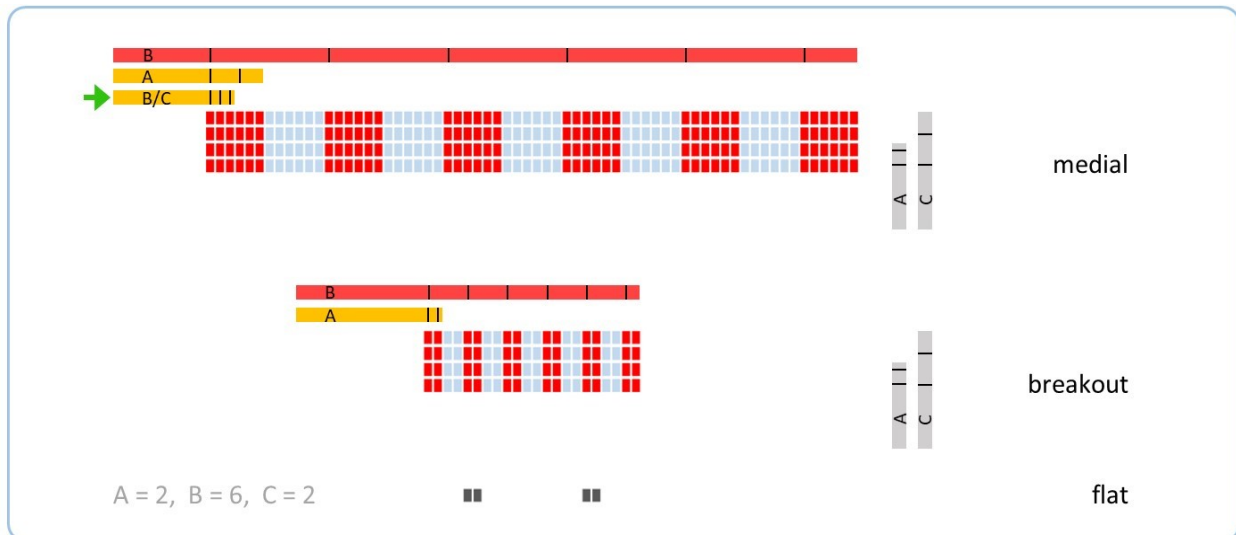
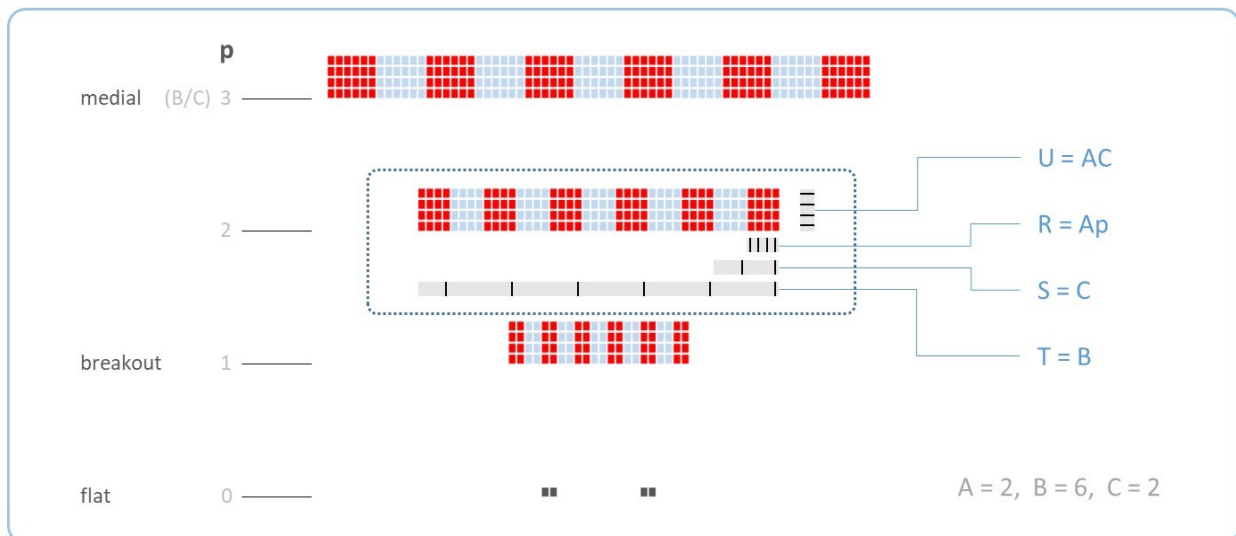


Figure 5.27, Inductive formulas



- At breakout a factor B/C is ranked *below* feature C, so there are a total of B closely-spaced slits in the same space which initially contained only C slits at the flat.
- At the medial, a factor of B/C is ranked *above* feature C, yielding are a total of B slits but at the same original period as at the flat.
- Spatially, the trend appears as a simple magnification of the pattern, similar to the far field.

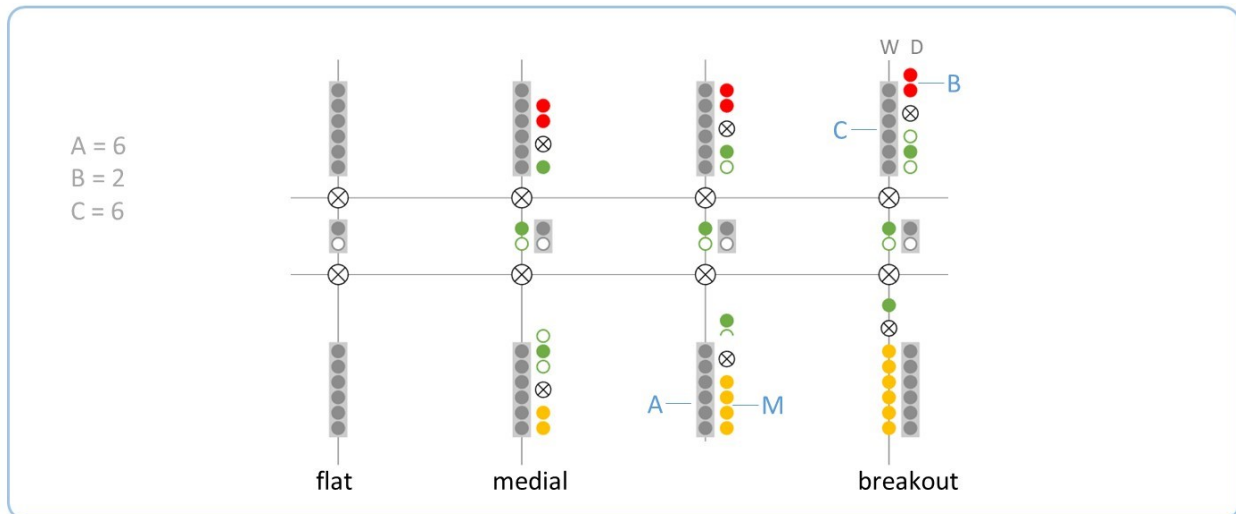
- Dark factor remains constant at C in this stage.
- While form grows, the number of slits remains constant at B.
- Depth remains constant at AC.
- Here in the early-breaking grating, the medial does *not* resemble the initial pattern; the texture and form are both wider. However, the array is the same as the initial array.

5.6 Breakout

5.6.1 Breaking case 1, late-breaking

- The formulas here are valid when texture sprouts by medial, i.e. when $AB \geq C$

Figure 5.28, Feature diagram



- At the medial $M < A$, so A is wide and M is deep (rule 4).
- M grows until breakout, where $M = A$ and M and A exchange inclination (rule 4). This is similar to the early elbow case 1, or to the simple beam.
- C is wide and B is deep (rule 4).
- From medial to breakout, B rises in rank from the bottom of C to the top of C. However, the inclinations do *not* change because the sizes of B and C remain constant, and all of B always shares a rank some factor of C.

Figure 5.29, Spatial-symmetry diagram at endpoints

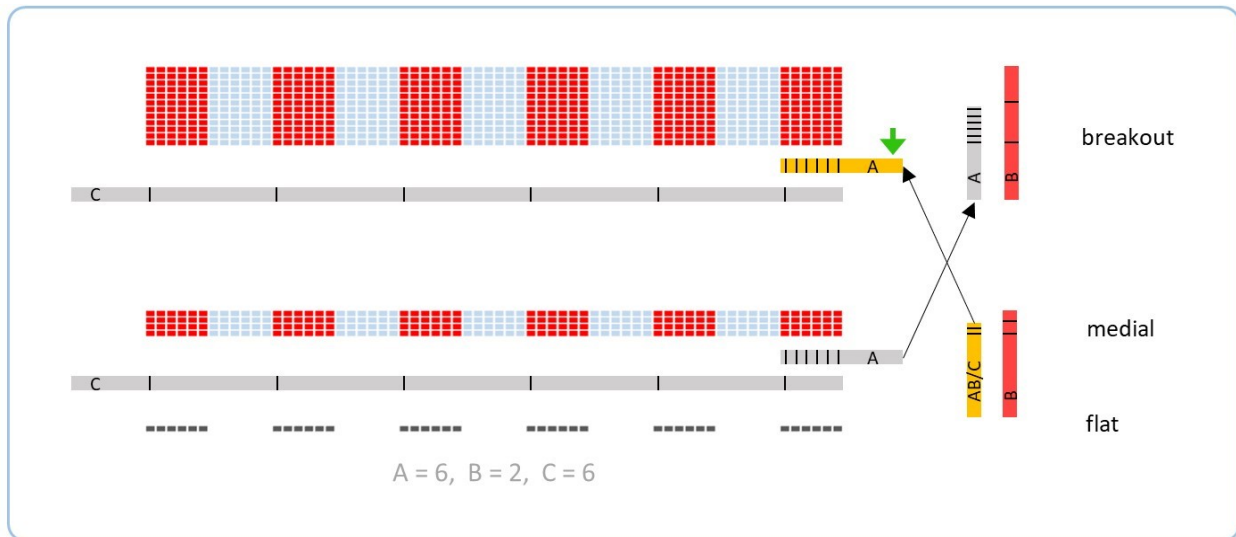
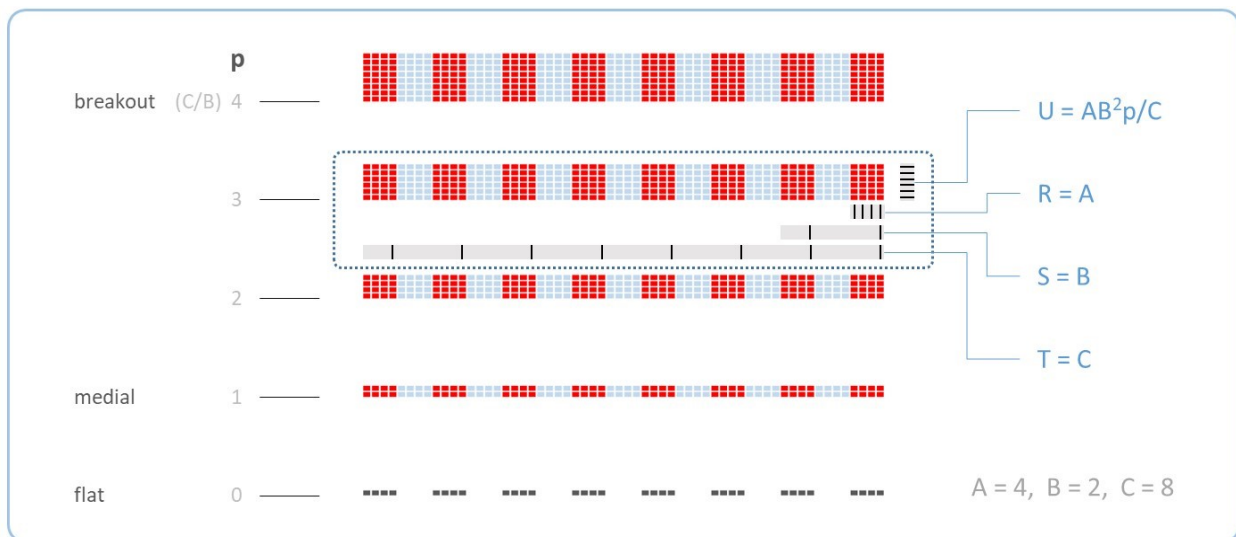


Figure 5.30, Inductive formulas

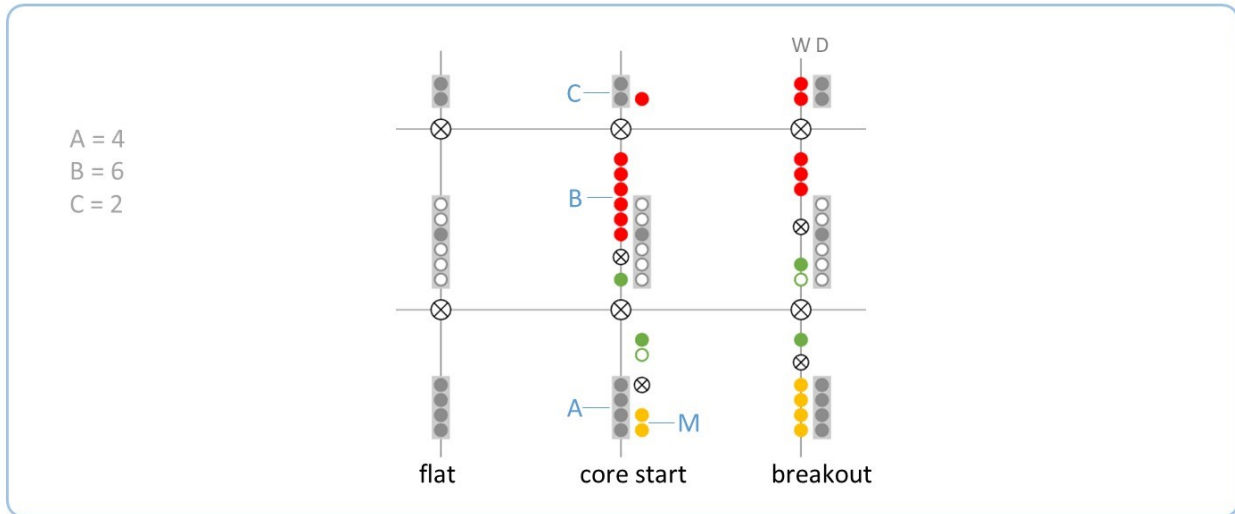


- Pattern texture, array, and form all remain constant, while depth increases. Note that this trend counts only the planes at integer values of p ; these are the late revivals. In between revival planes are fractional revivals, which do *not* follow the same trend.

5.6.2 Breaking case 2, early-breaking

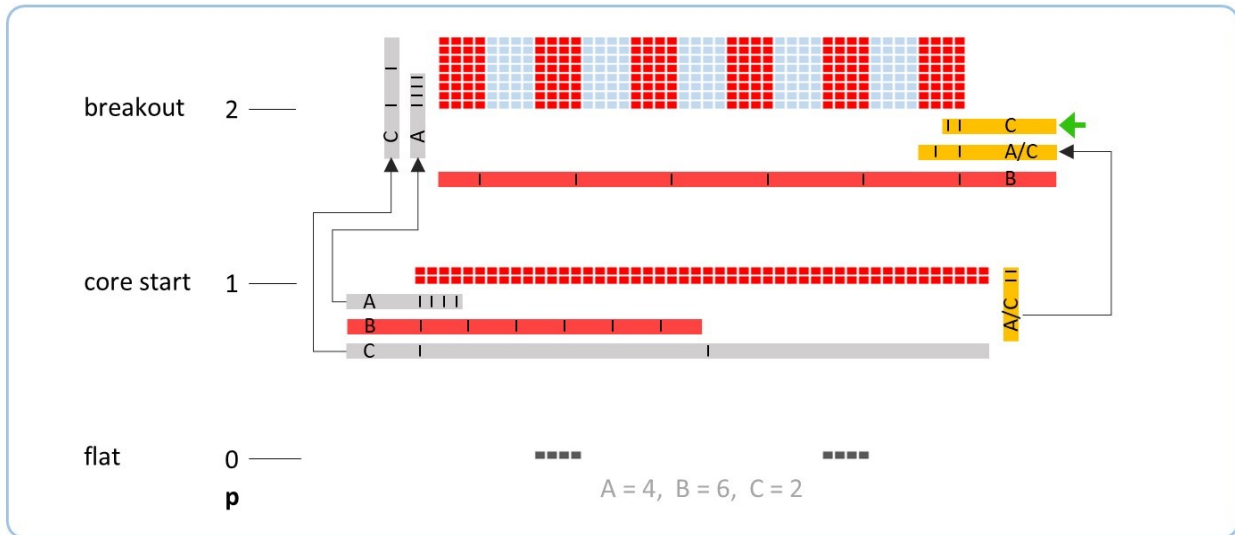
- In the early-breaking case, the breakout plane occurs *before* the medial. Therefore, this case is presented out of its actual physical order.
- The formulas here are valid when texture sprouts by core start, i.e. when $A \geq C$.

Figure 5.31, Feature diagram



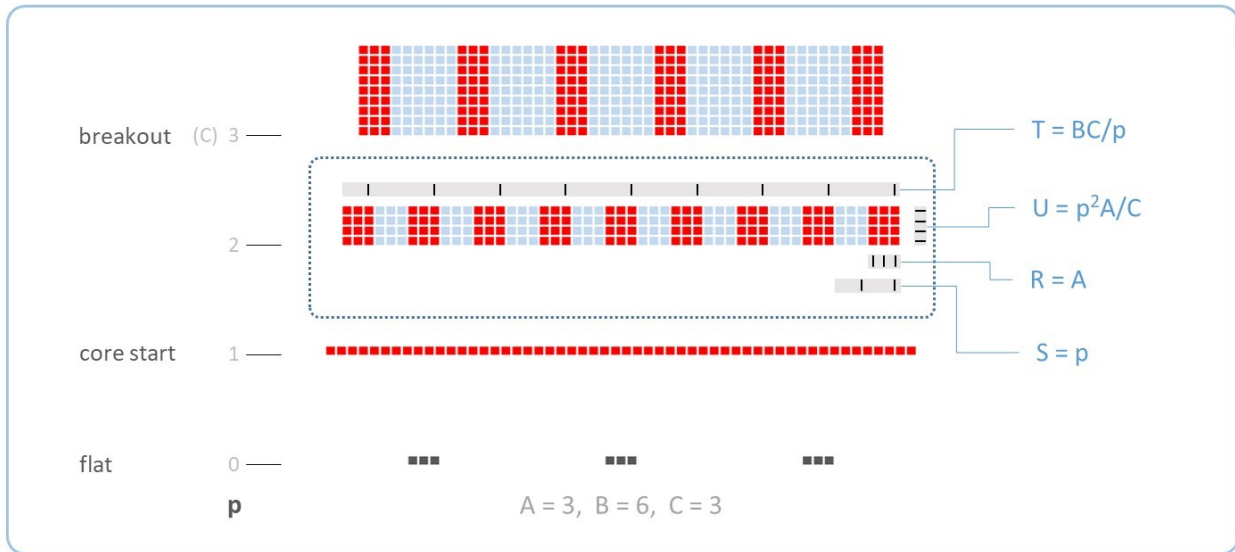
- At core start, B and C do not share a rank (single patch is trivial). B is wide (rule 2); C is also wide (rule 1).
- At breakout, C ranks with one factor of B. Smaller feature C is deep; larger feature B is wide (rule 4).
- Lower-ranking features M and A provolve just as in the previous (late-breaking) case.

Figure 5.32, Spatial-symmetry diagram at endpoints



- While the shine grows by a factor of C, the depth increases by C^2 because it occurs in two different modes, as feature A and feature C both provolve to depth.

Figure 5.33, Inductive formulas

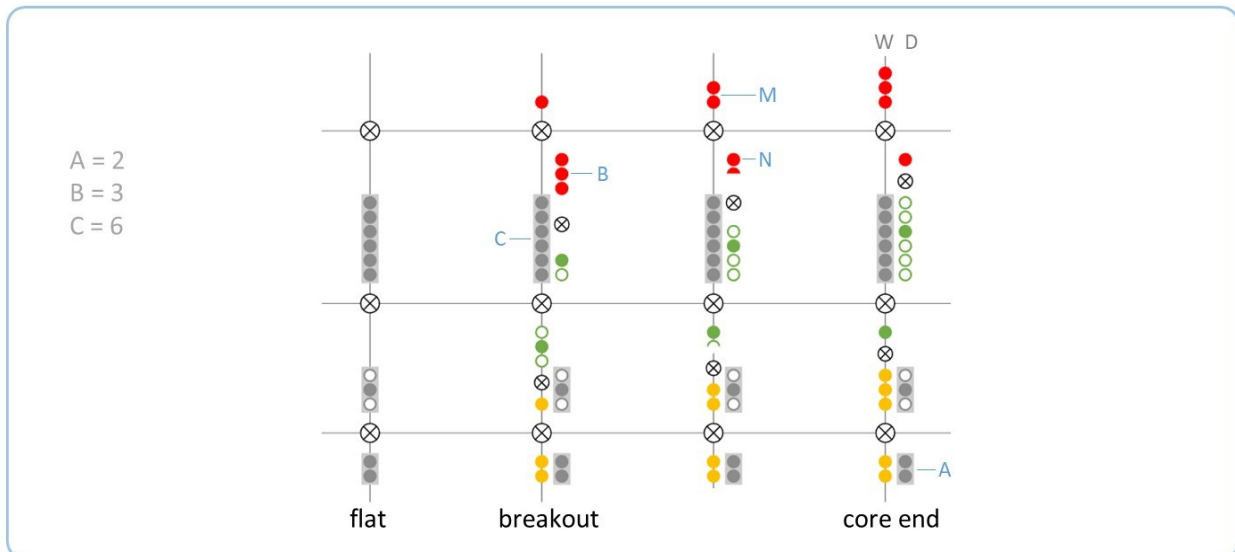


- Pattern texture and form remain constant, while pattern array expands. Number of slits decreases.

5.7 Core end

5.7.1 Breaking case 1, late-breaking

Figure 5.34, Feature diagram



- B breaks into 2 factors: factor N ranks at the top of C, while factor M ranks above C.
- Because B is smaller than C, overlapped factor N is deep (rule 5).
- Factor M is wide, independent of factor N (rule 5).

- From the flat up all the way up to breakout, A was wide; this manifested as a constant pattern texture of width A during early, fractional, and late revivals. After breakout, pattern texture expands.
- At core end, the only depth is glow feature A. At no other rank is there both bright shine *and* bright glow at the same rank.
- There is also no rank at which there is both dark shine and dark glow; so, no dark space is observable.

Figure 5.35, Spatial-symmetry diagram at endpoints

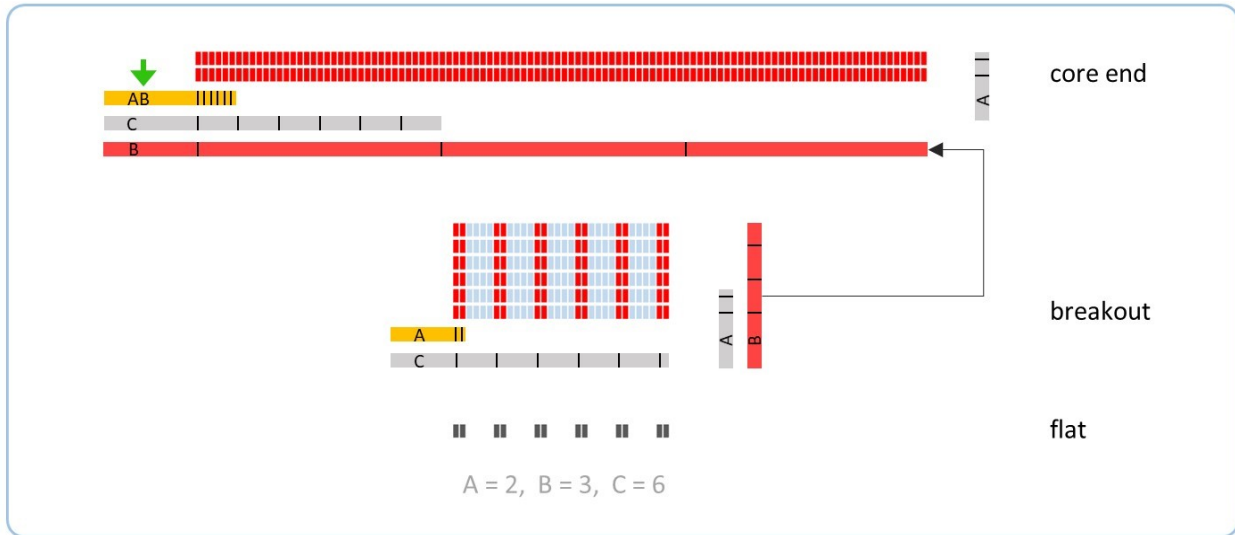
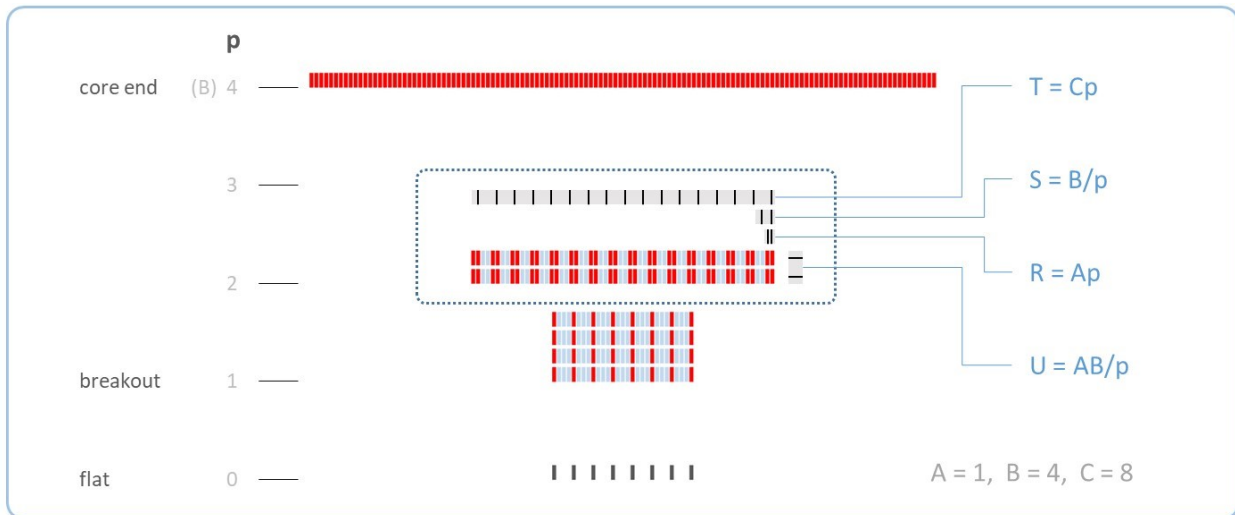


Figure 5.36, Inductive formulas



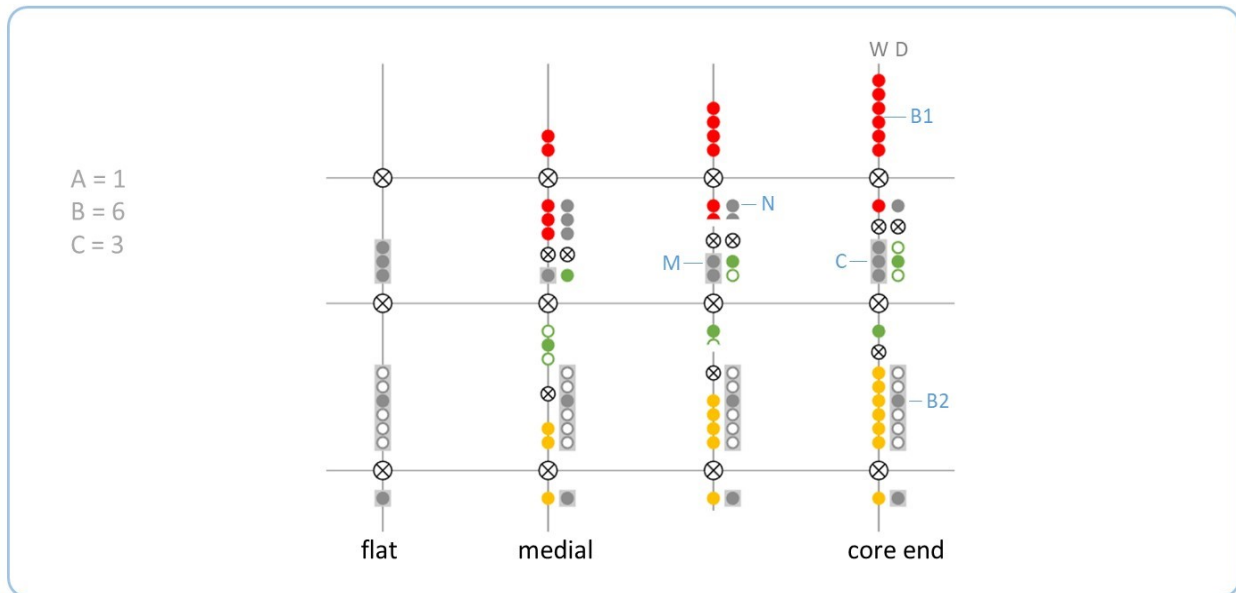
- Wide-inclined area increases by a factor of B^2 from two growth modes: First, the dark factor decreases from B to 1 as shine texture grows wider, filling the interstitial dark space. Second, the pattern form (overall size) expands as by a factor of B as feature B provolves from depth to width.

- Pattern array remains constant.

5.7.2 Breaking case 2, early-breaking

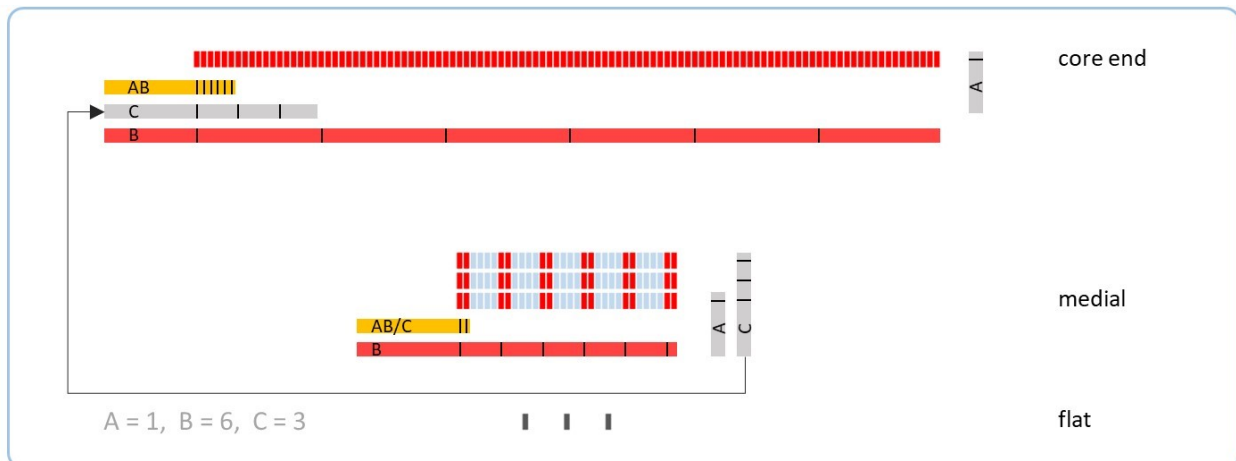
- While the core end plane is the same for both late- and early-breaking cases, the stage leading up to core end is different between the two cases.

Figure 5.37, Feature diagram



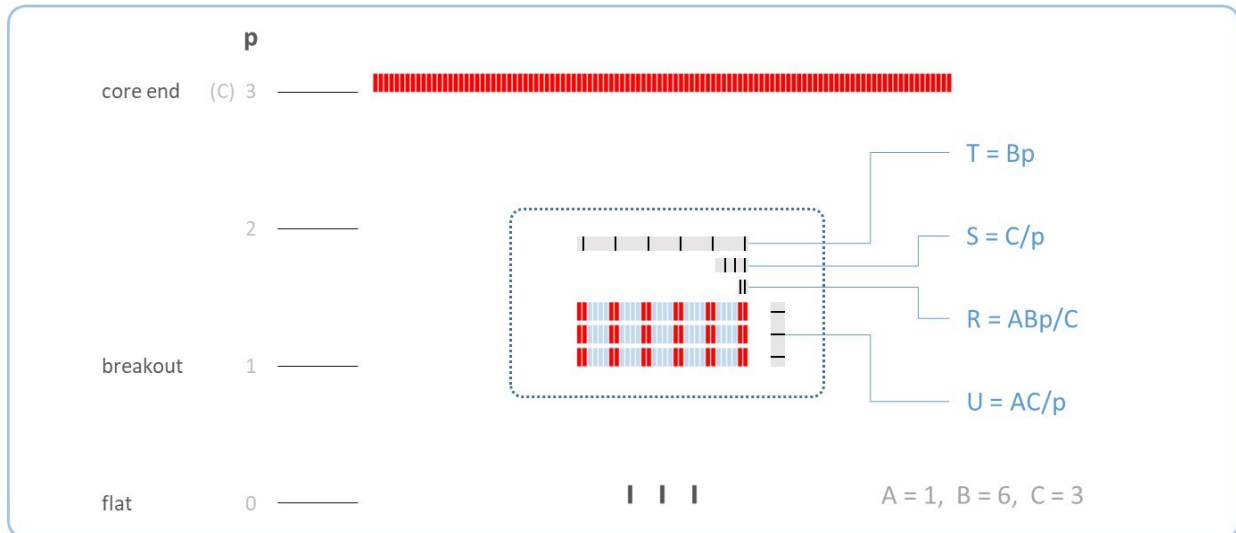
- B1 and C share a rank at the medial. B1 is larger so it is wide, while C is deep (rule 4).
- When B1 rises in rank, it overlaps only factor N. N remains deep, while factor M provolves wide (rule 5).
- B2 ranks with both bright and dark shine. It is deep in all cases (rule 2, rule 3).
- Dark shine rises to rank with C, and provolves deep (rule 2).

Figure 5.38, Spatial-symmetry diagram at endpoints



- Dark shine is not observable at the core end. However it still exists, and will become observable again in the next stage.

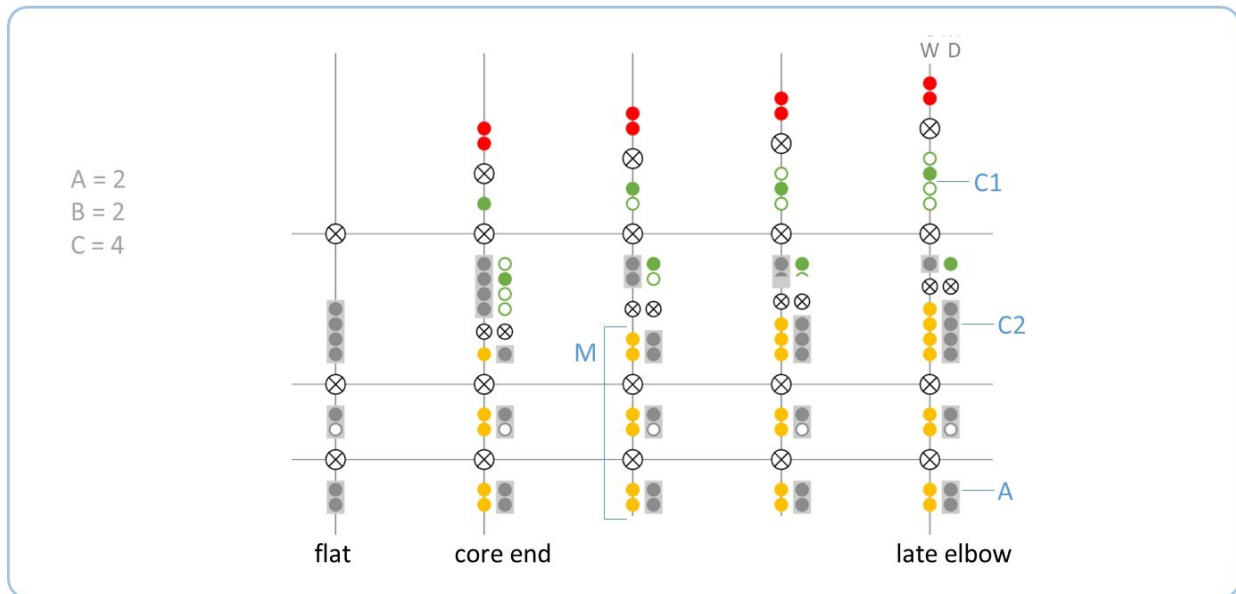
Figure 5.39, Inductive formulas



5.8 Late elbow

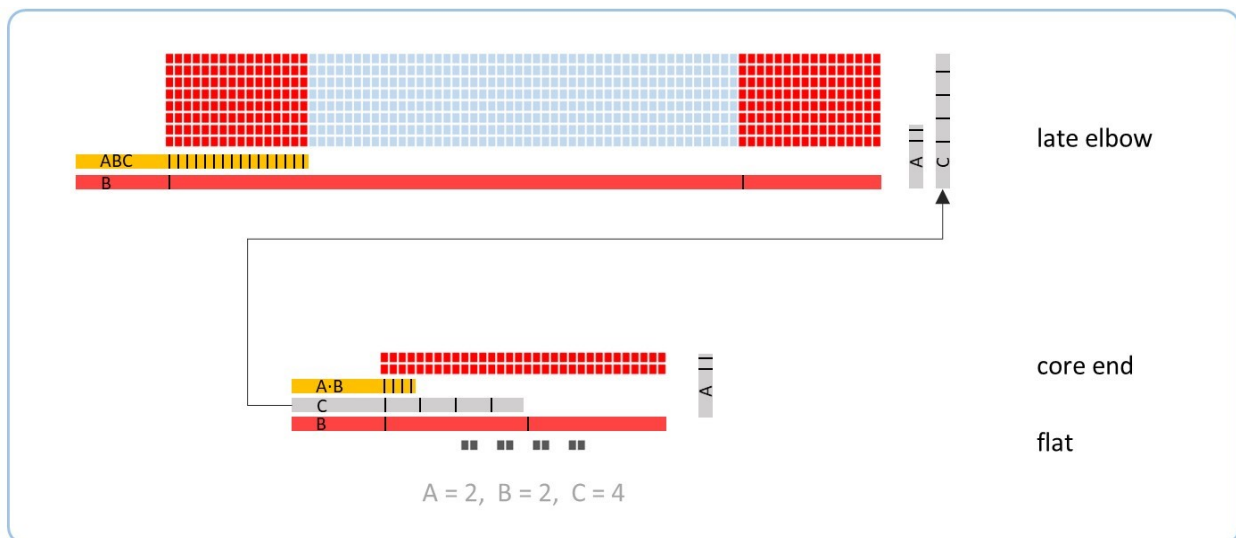
- This is the final stage in which discrete inclinations change.
- From the late elbow onwards, all glow features are deep while all shine features are wide. This is the exact reverse of the inclination at the flat; it is the Fourier transform of the initial pattern.
- Beyond the late elbow, the shine texture continues to grow. The depth remains constant, while the width continues to expand indefinitely, preserving the observable pattern except for a uniform magnification.

Figure 5.40, Feature diagram



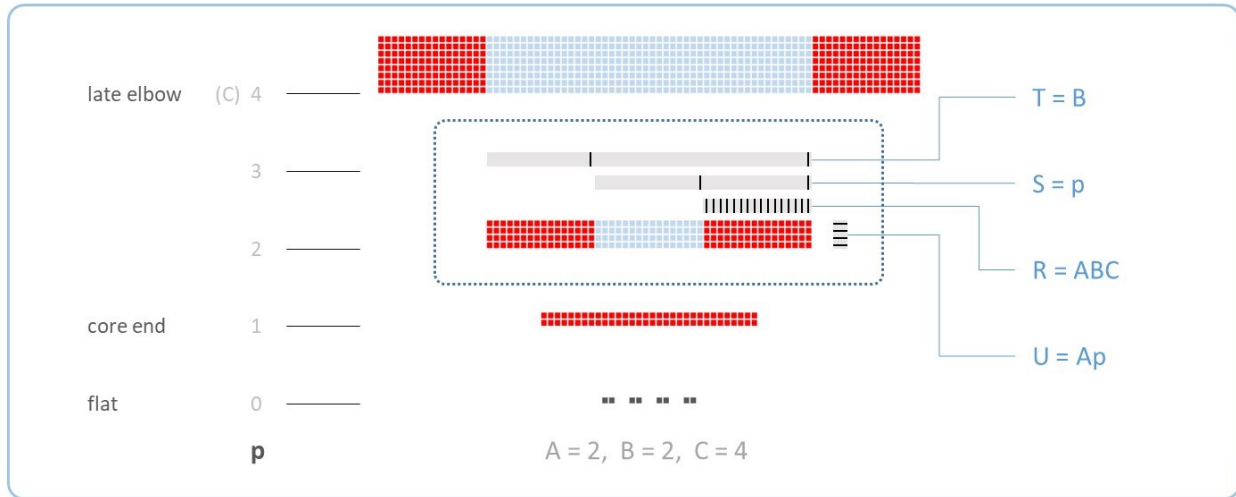
- M is already larger than C2 by the core end (usually, though not in every case), so M is wide after the core end. As M grows and rises in rank, C2 provolves deep (rule 5, rule 6).
- C1 is deep at core end because it is dark (rule 2), but as it rises in rank it provolves wide (rule 3) and becomes observable as the dark space in between the far-field orders.

Figure 5.41, Spatial-symmetry diagram at endpoints



- A simple beam of width ABC gains depth up to its elbow, then stops but begins to expand in width. The far-field orders are similar in width at the late elbow; however, the depth is only AC, *not* ABC as would be expected in a simple beam of the same diameter. This 'missing' factor of B appears instead as the number of distinct orders at the late elbow.

Figure 5.42, Inductive formulas



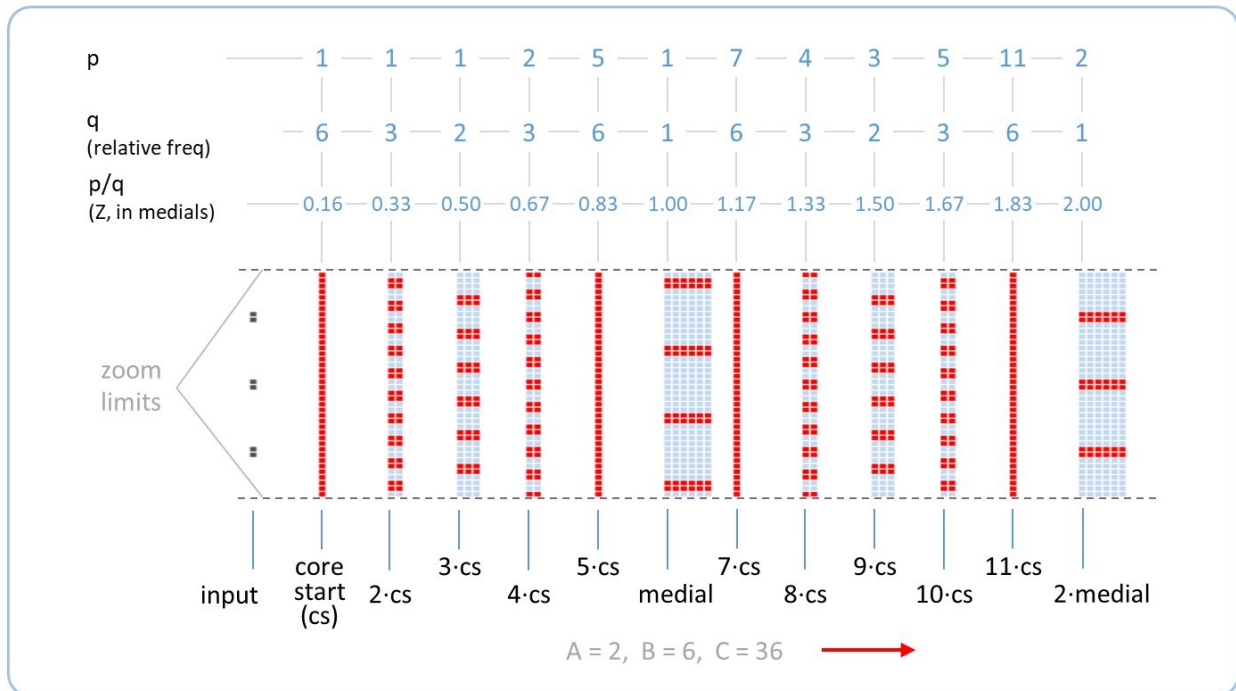
6 Fractional Talbot planes

For the late-breaking grating, the foregoing analysis considered only the planes that exemplify the idealized trend. However, these planes constitute only a subset of the *fractional Talbot images*, which occur at many other planes between the core start and breakout. The patterns in these planes have the same texture and form as the input pattern, but the array is smaller by a whole-number divisor. These occur when

$$Z = \frac{p}{q} \cdot \frac{d^2}{\lambda} = \frac{p}{q} \cdot Z_{\text{Elbow}}$$

where d is the period of the grating, and p and q are all possible coprime integers¹⁰. Values Z , d , and λ have units of length. The value q at any plane is the *relative* spatial frequency, compared to the input pattern. Our spatial-symmetry diagram algorithm reproduces these patterns at any plane whose Z -distance is an integer multiple of the core start distance A^2B . An example is shown in Figure 6.1.

Figure 6.1, Fractional Talbot images



Many other authors have computed results similar to these^{11,12,13,14,15}. However, all those models employed conventional wave optics to model interference between sources. Remarkably, FO does not rely on wave optics at all; it does not use such concepts as phase or interference. Yet, it computes the same results.

The region from core start to breakout, where these planes occur, coincides with the growth of dark shine. Accordingly, the total symmetry does not increase; rather, it oscillates between width and depth, while their product remains constant.

7 Beams and revivals

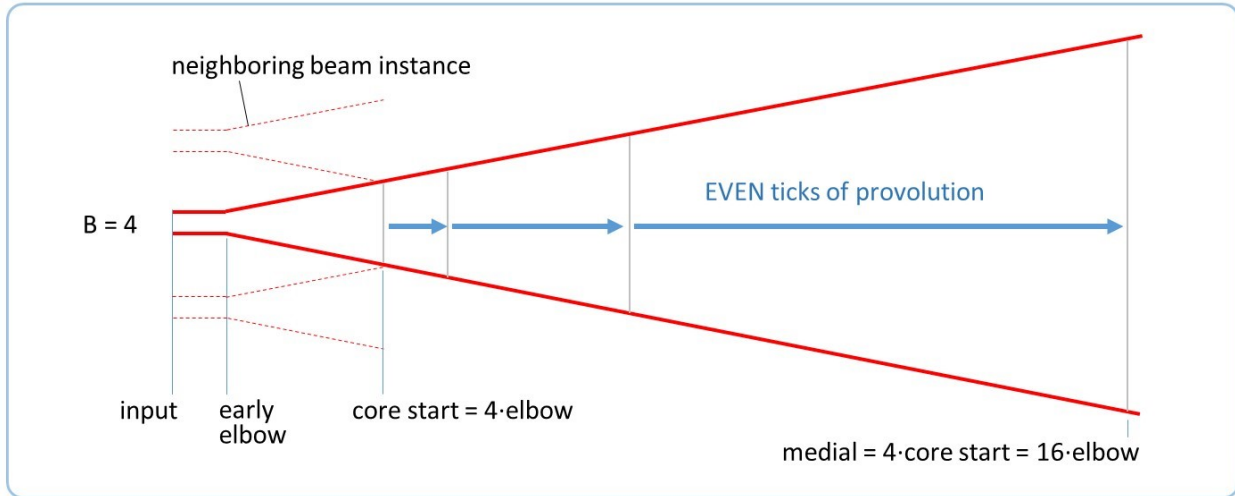
7.1 Early revivals

In reference 2, we quantified early revivals in terms of patches in the feature diagram. However, we can also quantify them in terms of the inclination of the *early beam*, which was also introduced in the same reference. The early revivals begin with the core start and end with the medial, and are spaced equidistantly in inclination, with the spacing

$$\Delta i_{\text{earlyBeam}} = \frac{1}{B^2}$$

Where B is the size of the dark glow feature at the input plane; alternatively, B is the number of order beams in the far field. This makes sense in terms of the rules for far-field beam provolution⁵. The glow impurity is 1 at the elbow, and falls to $1/B$ at B times the elbow distance (core start) and $1/B^2$ at B^2 times the elbow distance (medial, see Figure 7.1).

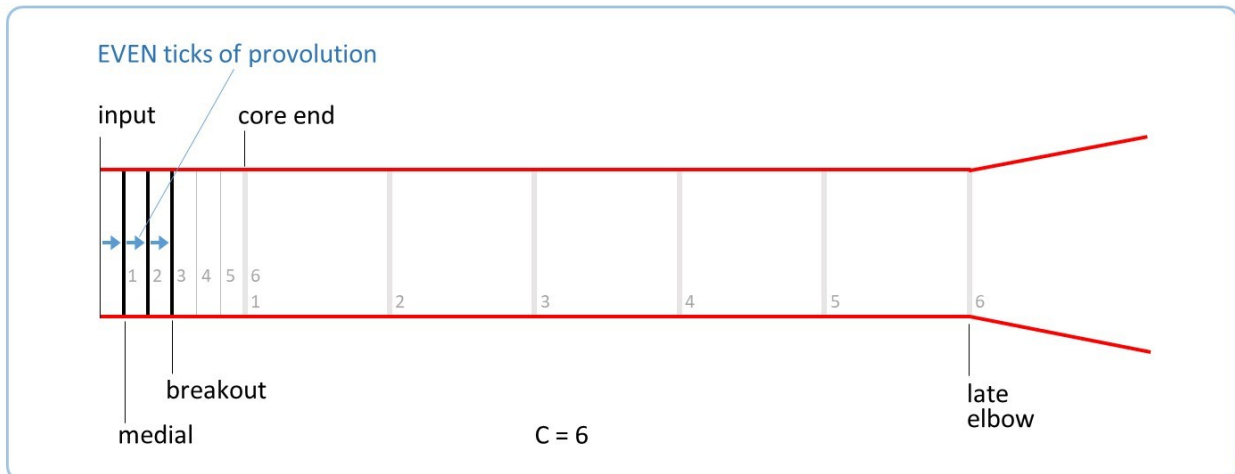
Figure 7.1, Early revivals and early beam inclination



7.2 Late revivals

The late revivals can also be quantified in terms of the inclination of the *late beam*. Figure 7.2 shows that the late beam's near field may be divided into C (here, $C=6$) equal lengths of Z_{coreEnd} , and that Z_{coreEnd} itself may be divided into C equal lengths of Z_{medial} . At each step of Z_{medial} up to breakout, a late revival occurs. Note that the total number of late revivals is not C , but rather the ratio C/B .

Figure 7.2, Late revivals and late beam inclination



Because the provolution in the near field occurs linearly with Z, the ticks of inclination are spaced according to

$$\Delta i_{\text{lateBeam}} = \frac{1}{C^2}$$

Where parameter C is the number of instances of the early beam at the flat, or the dark factor in the FT plane.

Note the similarities and differences between the early and late revivals. Their provolutions are counted according to two different beams, but in both cases, a total provolution of 1 is divided by the square of the number of slits that the beam contains, in the plane where it plays the role of the form.

8 Continuous feature diagrams

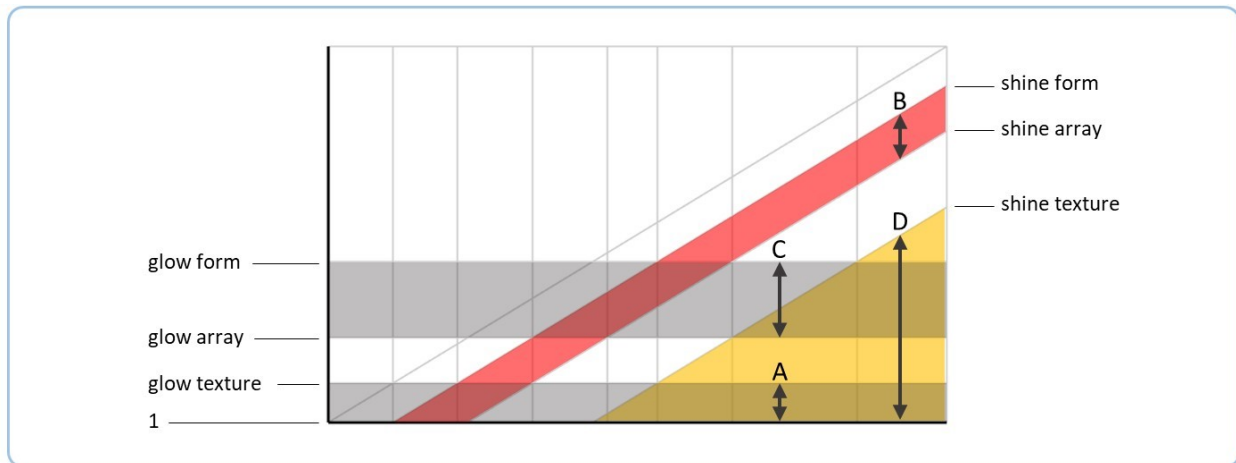
8.1 Continuous features

In earlier chapters and in earlier work, we computed pattern depths and shape widths using arrays of discrete cells. Those algorithms can accept only integer feature sizes. However, we can also generalize to sizes of all real numbers greater than or equal to 1, by using *continuous features*. Not only will this let us handle additional cases, it also obviates the need for special rules to handle different sprouting cases. It also gives us a consistent, formulaic procedure that does not rely on inductive formulas.

The main drawback of continuous features is that without the spatial diagrams computed by the cell-array methods, a new user may find it difficult to grasp the physical meaning of the feature diagram.

Figure 8.1 shows a log-log plot of glow and shine shapes, as drawn in reference 4. However, it can also be interpreted as a feature diagram. Rather than interpret each line as a size, we can interpret the bands between shapes as features ranked in a chain. In this case, we do not color the dark features because they do not affect the quantities we wish to compute.

Figure 8.1, Shapes and features



One shortcoming of the continuous feature diagram is that it does not indicate the inclination of the features.

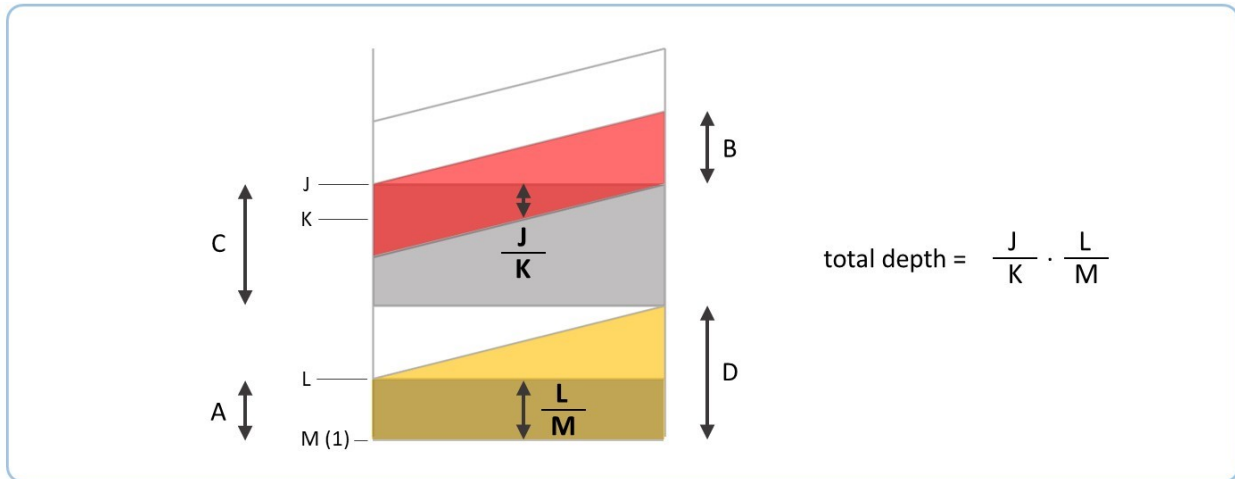
The details of all the following calculations can be found in the companion code, in the file *continuousFeatures.m* and its references. The file *inductive_vs_continuousFeatures.m* compares these results against those from inductive formulas; the test results are also included in pdf format and show an exact match.

8.2 Depth

Depth exceeds 1 whenever bright glow and bright shine share a common rank. In terms of Figure 8.1 above, this occurs when colored bands overlap.

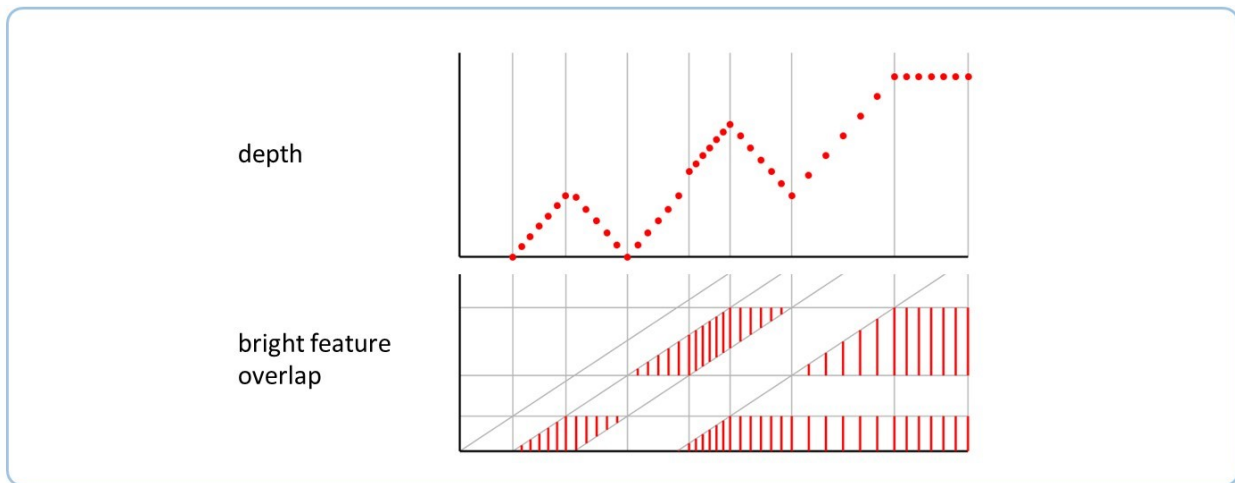
Figure 8.2 shows the details of the calculation in one plane. The overall depth consists of two factors: one from the overlap of B and C, and a second from the overlap of A and D. For each pair, the depth factor is the ratio between the highest and lowest points of the overlap. The lowest possible point is at 1, i.e. a single wavelength – lower features have not yet sprouted.

Figure 8.2, Calculating depth in one plane



A typical depth progression is shown in Figure 8.3. These progressions vary from one case to another, and a detailed analysis is beyond the scope of this work.

Figure 8.3, Typical depth progression



8.3 Width

If depth is the intersection ('and') between two bright features, then width is the union ('or'). If there at least one bright feature at a given rank, the rank appears bright to the observer; if all features at one rank are dark, it appears dark.

While depth is a single number, the width consists of three shapes – form, array, and texture. From these, it is also easy to calculate the parameters R, S, and T used in the inductive formulas. It is easy to deduce the shape sizes from the feature diagram, but the algorithm follows a precise formula which is implemented in the companion code:

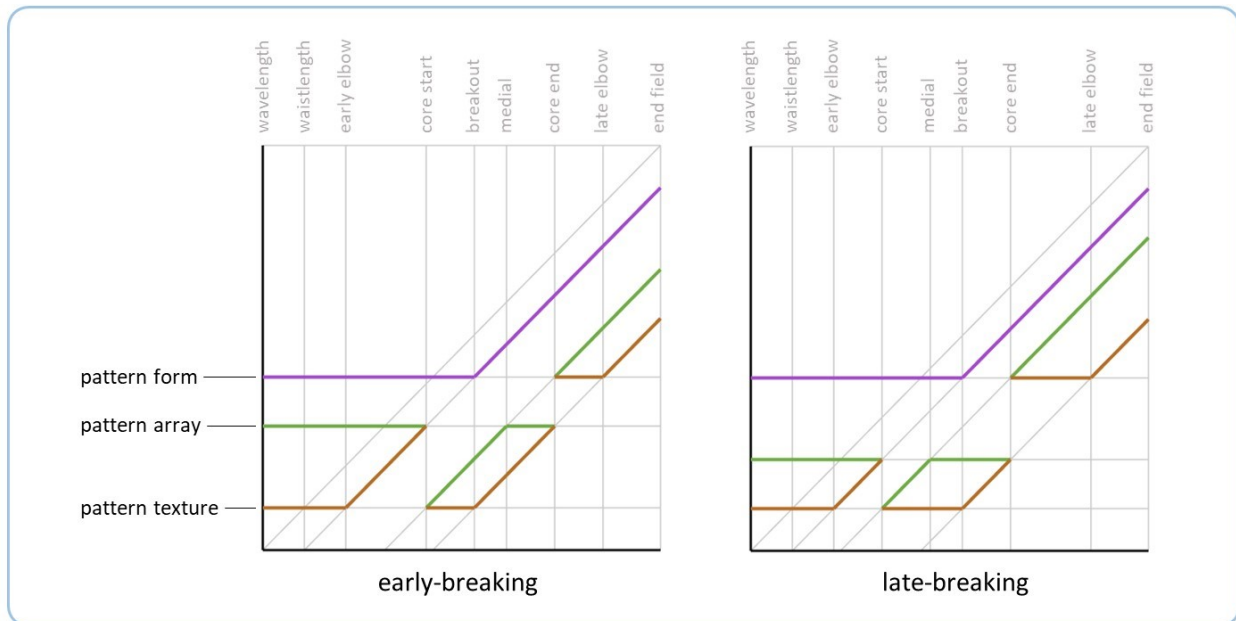
The pattern form is the larger of glow form and shine form.

If glow array and shine array do not overlap, then the pattern array is the larger of the two. If they do overlap, the pattern array is the smaller of the two.

If features A and B overlap, then the pattern texture is the larger of the two. If features C and D overlap, the pattern texture is the larger of those two. Otherwise, the pattern texture is the larger of A and D.

Figure 8.4 shows two examples of width shapes calculated from this method. One is late-breaking and the other is early-breaking; note that ignoring depth, these are the only two possible grating configurations.

Figure 8.4, Wide shapes in early- and late-breaking cases



9 Conclusion

We have used several related but distinct methods to compute the patterns in the critical planes of the grating. First, we have computed tracked- and stacked-shine diagrams. Second, we have proposed inductive formulas. Third, we have calculated patterns from continuous-shine diagrams using simple rules. Fourth, in an earlier work² we simply proposed ad-hoc empirical formulas for the patterns. All of these approaches have yielded closely-matching or identical results.

10 References

1. Mirsky, Paul L. A First Look at Feature Optics. <http://vixra.org/abs/1909.0157>, 2019
2. Mirsky, Paul L. Feature Optics and the Critical Planes of the Grating. <http://vixra.org/abs/1909.0185>, 2019
3. Mirsky, Paul L. Symmetry and Asymmetry in Feature Optics. <http://vixra.org/abs/1909.0184>, 2019
4. Mirsky, Paul L. Glow and Shine in Feature Optics. <http://vixra.org/abs/2005.0205>, 2020
5. Mirsky, Paul L. Provolution in the Feature-Optical Beam. <http://vixra.org/abs/2005.0221>, 2020
6. Ozaktas, H.M. and Mendlovic, David. Fractional Fourier transform as a tool for analyzing beam propagation and spherical mirror resonators. Optics Letters, Vol. 19, No. 21, 1994.
7. Ozaktas, H.M. and Mendlovic, David. Fractional Fourier Optics, J. Opt. Soc. Am. A, Vol. 12, No. 4, April 1995
8. Ozaktas, H.M., Zalevsky, Zeev, and Kutay, M. Alper. The Fractional Fourier Transform with Applications in Optics and Signal Processing. Wiley and Sons, 2001
9. Github repository at <https://github.com/paulmirsky/provolutionInGrating>
10. Wen, J., Zhang, Y., and Xiao, M. The Talbot effect: recent advances in classical optics, nonlinear optics, and quantum optics. Adv Opt Photonics 5, 83–130, 2013
11. Berry, Michael; Marzoli, Irene; and Schleich, Wolfgang. Quantum carpets, carpets of light. Physics world, June 2001
12. Latimer, Paul, and Crouse, Randy F. Talbot effect reinterpreted. Applied Optics, vol 31 no. 1, 1992
13. Latimer, Paul. Talbot plane patterns: grating images or interference effects? Applied Optics, vol 32 no. 7, 1993
14. De Chatellus, Hughues Guillet; Lacot, Eric; Hugon, Olivier; Jacquin, Olivier; Khebbache, Naïma; Azaña, José. Phases of Talbot patterns in angular self-imaging. <https://hal.archives-ouvertes.fr/hal-01165168>, 2015
15. Case, William B.; Tomandl, Mathias; Deachapunya, Sarayut; and Arndt, Markus. Realization of optical carpets in the Talbot and Talbot-Lau configurations. Optics Express vol 17 no.23, 2009